Water sorption properties of brewer's spent grain: A study aimed at its stabilization for further conversion into value-added products

Marcio Augusto Ribeiro Sanches, Pedro Esteves Duarte Augusto, Tiago Carregari Polachini, Javier Telis-Romero

Sanches, M. A. R., Augusto, P. E. D., Polachini, T. C., & Telis-Romero, J. (2023). Water sorption properties of brewer's spent grain: A study aimed at its stabilization for further conversion into value-added products. *Biomass and Bioenergy*, *170*, 106718.

https://doi.org/10.1016/j.biombioe.2023.106718

Water sorption properties of brewer's spent grain: A study aimed at its stabilization for further conversion into value-added products

Marcio Augusto Ribeiro Sanches[1*], Pedro Esteves Duarte Augusto[2], Tiago Carregari Polachini[1], Javier Telis-Romero[1]

[1]Food Engineering and Technology Department, São Paulo State University, Institute of Biosciences, Humanities and Exact Sciences (Ibilce), Campus São José do Rio Preto, São Paulo, 15.054-000, Brazil.

[2]Université Paris-Saclay, CentraleSupélec, Laboratoire de Génie des Procédés et Matériaux, SFR Condorcet FR CNRS 3417, Centre Européen de Biotechnologie et de Bioéconomie (CEBB), 3 rue des Rouges Terres 51110 Pomacle, France.

*Author to whom correspondence may be addressed. E-mail address: mar.sanches@unesp.br (Marcio Augusto Ribeiro Sanches).

HIGHLIGHTS

- Different brewery operations significantly affected the BSGs compositions.
- The GAB model best described the sorption isotherms in all conditions evaluated.
- Water binding properties were slightly hampered by the higher protein contents.
- The type of sorption isotherm of the BSGs was affected by temperature.
- Multi temperature sorption study provides useful thermodynamic functions.

ABSTRACT

Due to its high moisture content and perishability, the water adsorption isotherms, and thermodynamic properties of brewer's spent grain obtained from barley malt (BSGL) and wheat malt based (BSGW) were evaluated under storage and drying conditions. Chemically characterized BSGs were subjected to the static gravimetric method to experimentally obtain the water adsorption isotherms at ten temperatures (5–90 °C). As the best-fitted model ($R^2_{adj} > 0.9928$ e $\chi^2 \leq 0.0001$), the GAB parameters were used to determine the adsorption surface area, spreading pressure, and thermodynamic properties. At temperatures from 5–50 °C, the adsorption isotherms of BSGL and BSGW showed convex curves, typical of type III isotherms. However, at temperatures above 60 °C, the curves started to present typical type II isotherms with sigmoid-shaped sorption behavior. The equilibrium moisture content of BSGs increased with increasing relative humidity and/or decreasing temperature. The spreading pressure increased as the water activity and temperature increased, contrary to that observed for the adsorption surface area. Thermodynamic analysis showed that the net isosteric heat of adsorption, enthalpy, and differential entropy decreased as the equilibrium moisture increased. The compensation theory was confirmed, and its results indicated that the adsorption processes were enthalpy-driven. The positive values for Gibbs free energy indicated that the adsorption processes were not spontaneous, which may be related to the composition of BSGs in

terms of lipids and proteins. From an energy and stability point of view, a water activity of 0.4 is the ideal condition for the storage of BSGs.

Keywords: Agro-industrial byproduct; lignocellulosic biomass; Protein; Sorption isotherm; Stabilization; Model fitting.

1 INTRODUCTION

Although there is a growing trend for valorizing agro-industrial by-products as raw materials for different industries, there is a lack of work in the literature on the by-product properties over its processing conditions for stabilization - limiting the adequate and efficient design of the appropriate operations.

Beer is one of the most consumed and appreciated beverages worldwide [1]. On the other hand, brewer's spent grain (BSG) ends by turning into the main solid waste, representing 85% of the total by-products generated in the brewing industry [2]. BSG is made up of the solid part, such as husks and residual starchy endosperm, obtained after filtration of the wort, and the retained water. Representing about 20 kg of wet bagasse for every 100 L of beer produced [3], its composition varies with the beer formulations, in special the amount and type of malted cereal, and whether adjuvants were used during fermentation [4].

Currently, most part of BSG is still used only for animal feed or simply discarded [3], going in the opposite direction to sustainable food production and efforts to zero carbon emissions. In this sense, several studies have studied different potential applications of BSG, such as an alternative for plant-based protein sources [5] and the use of these proteins to stabilize emulsions [6], recovery of bioactive compounds [7],

bioethanol [2] or biogas [8] production, biodegradable packaging [9], xylitol synthesis [3], source of enzymes [10], and even the use of BSG as ingredient in processed foods [11].

However, one of the main challenges in recovering and using agroindustrial by-products is linked to its handling and stabilization [12]. The composition and high moisture content of BSG is one of the challenges for its management and use, as these factors make it susceptible to microbial growth and deterioration, in addition to the increasing transport cost [13]. In this way, BSG needs to go through a drying process to reduce its mass and volume – decreasing transport and storage costs, as well as prolonging its shelf life. Moreover, once the product is dried, adequate stored conditions ensure its availability and integrity for further applications.

For these purposes, some information is necessary for the correct dimensioning of equipment and drying processes, as well as to predict product stability. Water sorption isotherms are curves describing the relation between the food water activity (a_w) and its correspondent equilibrium moisture content (X_{eq}) at a given temperature, providing information on the availability and interactions between water molecules and the components of the solid matrix [14]. In addition to water molecules availability, the binding strength of water to matrix components can also be evaluated through differential enthalpy, while the number of available sorption sites at a specific energy level can be determined through differential entropy [15]. These two thermodynamic properties can still be correlated by the Gibbs free energy. Data about the adsorption surface area also provides important information about the binding properties of water with the solid matrix [16], while the spreading pressure can be understood as the driving force that provides diffusion in porous solids [17].

Despite being the subject of several published reports, research on the water adsorption properties of BSG has not yet been reported, this being the first study to

provide and compare data on the water adsorption isotherms and thermodynamic properties of BSGs from two different brewery processing (“Lager” and “Weiss” style). Therefore, this study aimed at determining and comparing the chemical composition, water adsorption isotherms, and thermodynamic properties of BSG from two different brewery processing, simulating both storage and drying conditions.

2 MATERIAL AND METHODS

2.1 Raw material and sample preparation

Brewer's spent grains (BSGs) were obtained from two different breweries. The present work was focused on studying BSG obtained from predominantly barley or wheat malts as the main malted cereals used in brewing. BSG "Lager" style (BSGL), was supplied by a brewery located in the city of Frutal – MG, Brazil. The beer produced was labeled as “pure malt”, made from a wort whose primitive extract comes exclusively from malted barley or malt extract, according to Brazilian legislation [18]. BSG "Weiss" style (BSGW), was supplied by a brewery located in the city of Blumenau – SC, Brazil. The beer produced was labeled as “wheat beer”, which may have a proportion of wheat malt greater than or equal to fifty-one percent, by weight, on the primitive extract, as a source of sugars, according to Brazilian legislation [18]. The by-products were collected and transported to the UNESP Physical Measurements Laboratory (São José do Rio Preto Campus). Three different batches of BSGL and BSGW were used.

The BSGs were dried in a convective tray dryer at 60 ± 2 °C, until equilibrium moisture was obtained, as performed in previous studies [12,13]. Afterward, the dried BSGs were ground in a rotor mill (model MA340, Marconi, Piracicaba, São Paulo, Brazil) and sieved in a 30 mesh sieve to obtain BSGs with granulometry lower than 595 μm.

2.2 Chemical composition of brewer's spent grains (BSGs)

Firstly, the two BSGs were characterized according to their chemical composition. Protein content was determined using the Kjeldahl method [19], with a conversion factor of 6.25. The mineral components were determined as ashes by incineration in a muffle furnace at 550 °C until white ash was reached [19].

Extractive content was analyzed by the Soxhlet method based on NREL/TP-510-42619 [20]. For this analysis, the biomass had to be subjected to extraction in water for 8 h, followed by extraction in ethanol for 24 h in a Soxhlet extractor.

The extractive-free material obtained after extraction with water and ethanol was subjected to acid hydrolysis to determine structural carbohydrates and lignin, according to the NREL/TP-510-42618 method [21]. The Klason lignin content was determined gravimetrically as an insoluble residue, according to Gomide and Demuner [22]. Acid-soluble lignin was measured by UV spectroscopy (Cary 50 Probe, Varian) at wavelengths 215 and 280 nm according to Goldschimid [23].

The determination of cellulose and hemicellulose contents followed the methodology adapted from NREL/TP-510-42618 [21]. These methods were carried out by the analysis in high-performance liquid chromatography (HPLC), in the Shimadzu Prominence chromatograph, using the filtered hydrolyzate obtained previously to the determination of insoluble lignin content of the sample (Klason method). Glucose, xylose, and arabinose monomers were quantified. The analysis conditions were: Phenomenex Rezex RPM-Monosaccharide column, lead stationary phase, mobile phase composed of 85% water and 15% acetonitrile, temperature controlled at 80 °C, the flow rate at 0.85 $mL \cdot min^{-1}$, for 18 min, with quantification by detector evaporative with light scattering (ELSD). When calculating the content of these constituents, the dilution made in the

process of quantification of insoluble lignin was considered. To convert the contents of monomers into the contents of cellulose, xylan, and arabinose, it was considered the contents of glucose, xylose, and arabinose, respectively. For cellulose content, the considered factor was 0.9, while for xylan and arabinan it was 0.88. Furthermore, the hemicellulose content was considered as the sum of the xylan and arabinan contents, as they represent the main constituents of this polymer [24].

Compositing results were expressed as mean ± standard deviation of five replicates.

2.3 Determination of the sorption isotherms

The water adsorption isotherms were analyzed using the static gravimetric method [25] at ten different temperatures, simulating storage (5, 10, 20, 30 e 40 °C) and drying (50, 60, 70, 80, and 90°C) conditions. For this, glass desiccators containing saturated solutions of LiBr, LiCl, $MgCl_2$, Nai, K_2CO_3, $Mg(NO_3)_2$, NaBr, KI, NaCl, $(NH_4)_2SO_4$, KCl, KNO_3 e K_2SO_4 were used to simulate environments with different relative humidities (RHs), which in equilibrium, are known as $a_w \cdot 100$. Temperatures that simulate storage conditions were provided by a BOD-type chamber (MA 830/A, Marconi, Brazil), and those that simulate drying conditions were controlled in an oven (MA035/2, Marconi, Brazil). The a_w values for each saline solution at different temperatures were obtained according to Labuza [26].

Approximately 3 grams of the BSGs were weighed (in triplicate) and placed in containers. After that, they were inserted into desiccators containing the different saturated saline solutions. The mass of the samples was weighed on an analytical balance (AUW220D, Shimadzu, Japan) until reaching constant mass, which took approximately 3 weeks. The X_{eq} of samples at each condition was calculated using the initial sample weight difference.

For prediction purposes, the mathematical models (Table 1) used in this study were chosen based on the study by Polachini et al. [12], for describing the sorption behavior of cassava bagasse. In addition, these models are commonly used to describe the experimental data and the mechanisms of sorption behavior agri-food products [13,27,28].

Table 1. Mathematical models fitted to the water adsorption isotherms data of the BSGs samples.

Model name	Model	Reference	Equation
GAB	$Xeq = \frac{X_m \times C \times k \times aw}{(1 - k \times aw)(1 + (C - 1)k \times aw)}$	Lomauro et al. (1985)	(1)
Halsey	$Xeq = (-h_1 \times ln(aw))^{-\frac{1}{h_2}}$	Halsey (1948)	(2)
Henderson	$Xeq = \left(-\frac{1}{H_1} \times ln(1 - aw)\right)^{\frac{1}{H_2}}$	Boquet et al. (1978)	(3)
Oswin	$Xeq = M \times \left(\frac{aw}{1 - aw}\right)^{N}$	Oswin (1946)	(4)
Peleg	$Xeq = k_1 \times aw^{n_1} + k_2 \times aw^{n_2}$	Peleg (1993)	(5)

C, *k*, k_1, n_1, k_2, n_2, *M*, *N*, h_1, h_2 H_1 e H_2 are constants of the models, X_m represents the monolayer moisture content (dry basis), X_{eq} is the equilibrium moisture content and a_w is the water activity.

These models were tested to describe the water adsorption isotherms of the BSGs. Fitting models to experimental data was performed by nonlinear regression using OriginPro 8.0 software (OriginLab Corporation, Northampton, MA). Fitting accuracy was analyzed through the determination coefficient (R^2_{Adj}), and chi-square (χ^2). Adjusted determination coefficients (R^2_{Adj}) close to 1, and χ^2 close to 0 indicate a great accuracy of the model to the experimental data.

$$R^2_{Adj} = 1 - \frac{n-1}{n-(k+1)}(1 - R^2) \quad (6)$$

$$\chi 2 = \frac{\sum_{i=1}^{N}(exp-pred)^2}{N-z} \quad (7)$$

n is the number of observations, *k* is the number of parameters in the model (excluding the constant), R^2 is the determination coefficient; exp are the experimental results; pred are the predicted results and N is the number of data values and z is the number of constants.

2.4 Adsorption surface area (ASA), Spreading pressure (Φ), and Thermodynamic properties

The adsorption surface area provides important information about the binding properties of water with the solid matrix. The adsorption surface area of BSG's was determined through Equation (8), as reported by [16].

$$ASA = X_m \frac{1}{M_{H2O}} A_{H2O} N_A = 3.53 \cdot 10^3 X_m \quad (8)$$

where ASA is the adsorption surface area ($m^2 \cdot g^{-1}$); N_A is the Avogadro's number ($6 \cdot 10^{23}$ moléculas$\cdot mol^{-1}$); M_{H2O} is the molecular weight of water (18 $g \cdot mol^{-1}$); A_{H2O} is the area of a water molecule ($1.06 \cdot 10^{-19}$ m^2); X_m is the moisture content of the monolayer ($kg \cdot kg^{-1}$ dry base).

Spreading pressure is the driving force that provides diffusion in porous solids. The spreading pressure was calculated from the equation (9) reported by [29]:

$$\Phi = \frac{K_B \cdot T}{A_m} \cdot \ln\left[\frac{1+c \cdot k \cdot a_w - k \cdot a_w}{1-k \cdot a_w}\right] \quad (9)$$

where Φ is the spreading pressure ($J \cdot m^2$); T is the temperature (K); A_m is the surface area of a water molecule ($1.06 \cdot 10^{-19}$ m^2); K_B is the Boltzmann constant ($1.38 \cdot 10^{-23}$ $J \cdot K^{-1}$); c and k are the parameters of the GAB model.

The net isosteric heat of adsorption is a thermodynamic property that describes the binding energy between the matrix and the water molecules as a function of the water content. It can be determined through the slope of the Clausius-Clapeyron equation (Eq. (10)), according to [30], as performed in previous studies [13,28].

$$\frac{\partial(ln\ a_w)}{\partial\left(\frac{1}{T}\right)}|_{Xeq} = -\frac{q_{st}}{R} \quad (10)$$

where q_{st} is the net isosteric heat of adsorption; T is the absolute temperature (K); R is the universal gas constant (8.314 J·mol^{-1}·K^{-1}). The water activity corresponding to certain equilibrium humidity was obtained through the model chosen to represent the adsorption isotherms of BSGs. As seen as the behavior of water adsorption can be represented through thermodynamic properties, the values of entropy (ΔS, J·mol^{-1}·K^{-1}) and differential enthalpy (ΔH, J·mol^{-1}) were obtained through Equation (11) using the same procedure used to determine q_{st}.

$$ln\ (a_w) = -\frac{\Delta H}{RT} + \frac{\Delta S}{R} \quad (11)$$

The Gibbs free energy (ΔG, J·mol^{-1}), which represents the free energy available to perform useful work and to assess the spontaneity of the process [16], was calculated using Equation (12) [30]:

$$\Delta G = RT \cdot ln\ a_w \quad (12)$$

Confirmation of a linear relationship between entropy and enthalpy variations is frequently used in the literature [12,13,28] to prove the theory of thermodynamical compensation, according to Equation (13):

$$\Delta H = T_B \cdot (\Delta S) + \Delta G \quad (13)$$

where, T_B is the isokinetic temperature (K), which represents the temperature at which all sorption phenomena occur at the same rate.

Another requirement to validate the theory of compensation is to compare the isokinetic temperature with the harmonic mean temperature T_{Hm} [31,32] given by Equation (14), where n is the number of isotherms.

$$T_{hm} = \frac{n}{\sum_{i-1}^{n}\left(\frac{1}{T}\right)} \tag{14}$$

To assess whether there is a statistically significant difference between the isokinetic temperature and the harmonic mean temperature, a confidence interval of $(1-\alpha)\cdot 100\%$ was calculated using Equation (15):

$$T_B = T_B \pm t_{m-2,\alpha/2}\sqrt{Var(T_B)} \tag{15}$$

In which,

$$T_B = \frac{\sum(\Delta H-\overline{\Delta H})\cdot(\Delta S-\overline{\Delta S})}{\sum(\Delta S-\overline{\Delta S})^2} \tag{16}$$

$$Var(T_B) = \frac{\sum(\Delta H-\overline{\Delta G_B}-T_B\Delta S)^2}{(m-2)\cdot\sum(\Delta S-\overline{\Delta S})^2} \tag{17}$$

m represents the number of data pairs (ΔH, ΔS), $\overline{\Delta H}$ the average enthalpy, and $\overline{\Delta S}$ the average entropy. A statistical significance α of 0.05 was used to calculate the confidence interval of 95%.

3 RESULTS AND DISCUSSION

3.1 Chemical composition

Table 2 presents the chemical composition obtained for BSGL and BSGW samples. Both BSGs had a high protein content (>21% on a dry basis (db)), with the highest ($P<0.05$) content found in the BSGW. The protein contents were higher or in the same order of other vegetables sources, such as pea that contains 20-25% of proteins (db) [33]; quinoa (*Chenopodium quinoa*) with approximately 13% of proteins (db) [34] or beans that contain 17.7-27.9% proteins (db) [35].

Table 2. Chemical composition of BSGL and BSGW (in g/100 g dry basis).

Component	BSGL*	BSGW*	P value
Proteins	21.489 ± 0.647 [b]	24.196 ± 0.215 [a]	0.0023
Extractives	8.368 ± 0.066 [a]	8.333 ± 0.101 [a]	0.6469
Ashes	3.674 ± 0.388 [a]	3.874 ± 0.317 [a]	0.5267
Cellulose	15.870 ± 0.784 [a]	15.416 ± 0.212 [a]	0.3868
Hemicellulose (Xylan)	23.629 ± 0.375 [a]	23.485 ± 0.091 [a]	0.5537
Hemicellulose (Arabinan)	4.851 ± 0.147 [a]	4.634 ± 0.079 [a]	0.0876
Insoluble Lignin	17.702 ± 0.284 [a]	16.757 ± 0.321 [b]	0.0187
Soluble Lignin	2.968 ± 0.049 [a]	2.934 ± 0.149 [a]	0.7288

In fact, because of that, the extraction and evaluation of the technological properties of BSG proteins have been studied [5,36] as an alternative plant-based protein source, although the industrial processing of BSG still needs a previous evaluation of physical and thermodynamical properties for an appropriate process design. In addition, the reuse of BSG proteins is in line with global trends toward the use of vegetable proteins for the human diet [37,38], as well as towards the integral use of renewable resources

(transforming by products into co-products and, thus, products, within the principle of circular economy). A small part of extractives (approximately 8.3%) and ashes (approximately 3%) also makes up the structure of these biomasses.

Another important part of the composition of BSGs is the content of cellulose, hemicellulose, and lignin, with potential application in biorefinery. BSGL and BSGW had the same content ($P>0.05$) of cellulose (approximately 15%), hemicellulose (Xylan approximately 23%; Arabinan; approximately 4%) and soluble lignin (approximately 2.9%). However, BSGL showed a higher ($P<0.05$) insoluble lignin content (17.7%) when compared to BSGW (16.7%). The complex matrix of lignocellulose is mainly formed by a thick structure of hemicellulose and lignin, which surrounds the cellulose molecules. The observed slightly higher content of insoluble lignin in BSGL may present an indicative about its lower reactivity and its slightly higher difficulty of removal from the complex. The high crystalline structure of cellulose, which is grouped into a matrix of polymers-lignin and hemicellulose, is the main difficulty regarding biomass recalcitrance. The fraction of crystalline cellulose directly impacts the efficiency of the hydrolysis process [10], requiring it to undergo pre-treatment steps. After undergoing hydrolysis, BSG proved to be an important source of sugar that can be used to produce bioethanol [10,39].

Moreover, the recovery of agro-industrial waste for the development of innovative bio-based polymeric materials [40,41] is a topic of growing importance. Moreirinha et al. [9] developed antioxidant and antimicrobial films based on BSG arabinoxylans, nanocellulose, and feruloylated compounds aiming at producing active packaging. These authors obtained films with antioxidant properties, antimicrobial activity against bacteria such as *Staphylococcus aureus* and *Escherichia coli*, and antifungal activity against *Candida albicans* – showing the potential application of BSGs in active food packaging systems. Edible films could be successfully developed by adding BSG proteins [42]. The

study of [43] demonstrated that the use of BSG as a functional filler in polypropylene matrix improved the degradability of the polypropylene matrix, resulting in more eco-friendly materials.

Other recent studies have shown interesting applications such as the use of BSG as carbon source for itaconate production with engineered *Ustilago maydis* after hydrothermal and enzymatic pre-treatments [44]; BSG liquor as a feedstock for lactate production with *Lactobacillus delbrueckii* subsp. *lactis* [45]; microwave pre-treated BSG for biobutanol production [46], among other value-added products [4]. These studies reinforce the potential of this by-product, generally considered waste, to be used as raw material in biorefinery processes with a wide range of industrial applications.

3.2 Water sorption isotherms

Figure 1 shows the changes in equilibrium moisture contents (X_{eq}) of BSGL and BSGW as a function of water activity (a_w) under storage and drying conditions.

Figure 1. Water adsorption isotherms of BSGs with the fitted GAB model at temperatures that simulate storage and drying conditions (points are experimental data; vertical bars are the standard deviation).

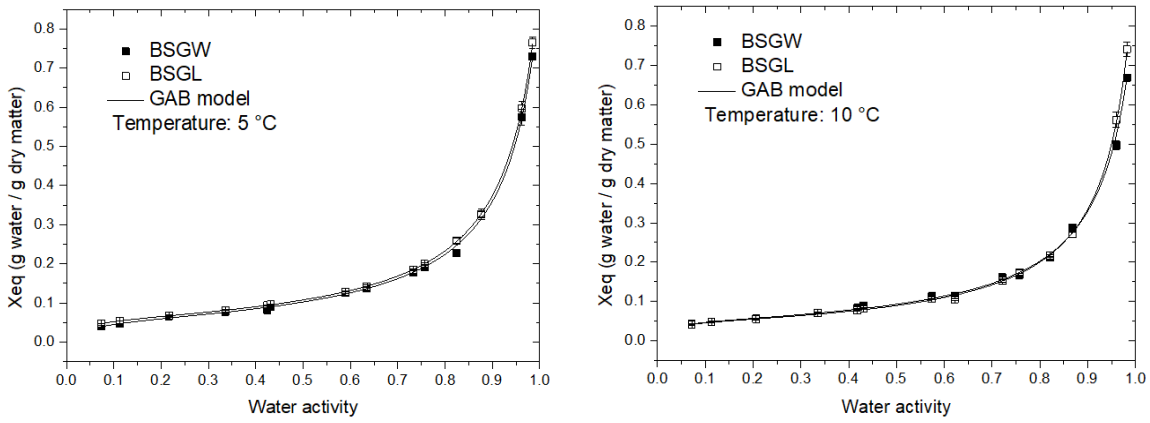

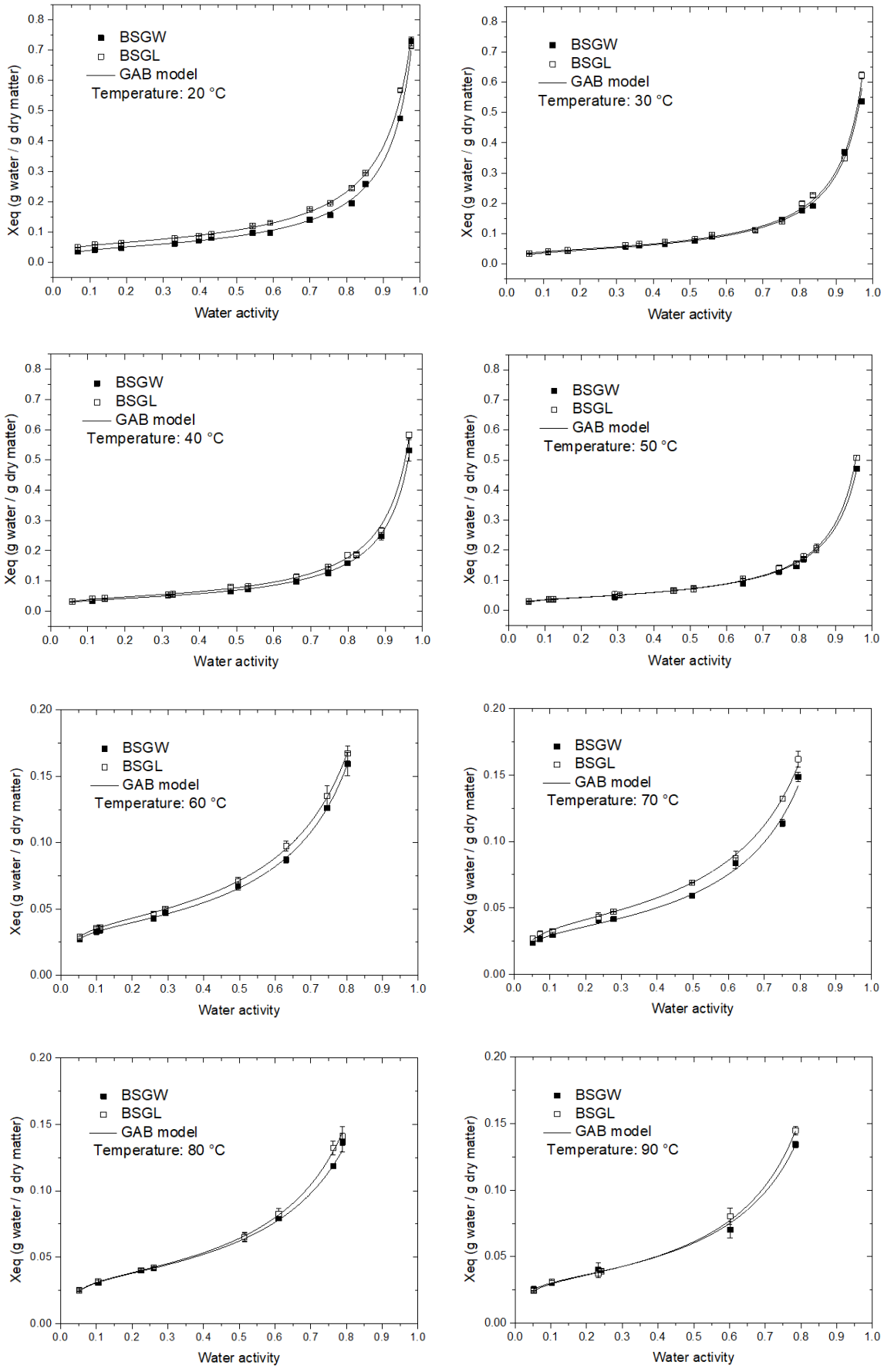

BSGL = Brewer's spent grain "Lager" style; BSGW = Brewer's spent grain "Weiss" style.

The values of X_{eq} and a_w (Supplementary Material - Table S1) ranged from 0.0236-0.7648 g of water·g^{-1} of dry matter and 0.0520-0.9848, respectively. Analyzing the data of X_{eq} and a_w at the same temperature, it is noted that X_{eq} increased because of the increase in a_w. On the other hand, it is possible to observe that in the same a_w, the X_{eq} decreased with increasing temperature. This behavior is probably related to the increase in the kinetic energy and the excitation state of the water molecules due to the increase in temperature, which probably reduced the attractive forces between the water molecules and the binding sites of the solid matrix. It makes easier their separation from the binding sites [25], thus promoting a reduction in the moisture content.

Figure 1 also shows higher X_{eq} values in the BSGL isotherms compared to BSGW ones, at almost all temperatures studied, mainly in regions of water activity close to 1. This demonstrates that the BSGL presented a greater water uptake capacity when compared to the BSGW. It can be a consequence of the higher protein content observed for BSGW when compared to BSGL. BSG proteins have a high content of hydrophobic amino acids (barley hordein and glutelins such as phenylalanine, valine, leucine, isoleucine, and methionine), as reported by [36]. In this sense, the greater amount of these nonpolar components may have hindered the water adsorption phenomena in the BSGW, reflecting in lower X_{eq} values.

The shape of the adsorption curves of BSGL and BSGW (Figure 1) were similar at each temperature studied. At temperatures from 5 to 50 °C, the adsorption isotherms of BSGL and BSGW showed convex curves, typical from type III isotherms from Brunauer classification [47]. These types of isotherms are commonly found for starchy and/or high-sugar products [25]. However, at temperatures above 60 °C, there was a slight change in the behavior of the sorption curves of BSGs. The curves started to present a typical behavior of type II isotherms [47], with sigmoid-shaped sorption. According to Mathlouthi [47], water sorption isotherms are generally described by three different

regions: (1) the region with a_w < 0.3 is composed of the monolayer moisture, which is strongly bound to the non-aqueous constituents of the matrix, through ionic bonds, and is not available for the growth of microorganisms nor enzymatic reactions; (2) the region with a_w between 0.3 and 0.7 is composed of the vicinal water, which presents an almost linear behavior and represents the next layer of water adjacent to the water of the monolayer; (3) the region with $a_w \geq 0.7$ presents water molecules that are less strongly bound to the non-aqueous components of the matrix, and that are available for chemical, enzymatic and microbiological reactions.

This changing behavior in the isotherms shape may be related to the gelatinization temperature of the residual starch present in BSGs. The adsorbed moisture in the matrix penetrated the amorphous regions of the granules, and above 60 °C in the presence of water, the intermolecular hydrogen bonds are broken down, releasing amylose and amylopectin chains, and resulting in the loss of crystalline zones [49]. The dispersion of such polysaccharides may have decreased the steric hindrance for water binding in comparison with non-gelatinized starch granules, making the transition from the second region of multi-layered moisture content towards the free water molecules zone slightly easier.

However, regardless of the isotherms type, the adsorption curves of BSGs showed an abrupt adsorption of water from the range of $a_w \geq 0.7$, which is probably related to the chemical composition of these materials, such as lignin, cellulose, hemicellulose, which have hydrophilic structures capable of water absorption [50]. In fact, similar adsorption curves have been reported for other lignocellulosic materials, such as cassava bagasse, papaya seed, and different types of wood [12,13,51].

Together with the composition, the water relations reinforce BSGs are easily degradable materials, whose processing (as drying or refrigeration) is needed for stabilization before any other step of valorisation. The sorption isotherms were then

evaluated through different models (Table 1), to provide ready-to-use information for further processing developments and thermodynamic analysis. Among the evaluated models, the GAB and Peleg models presented lower values of χ^2 and R^2_{adj} closer to 1 at all the evaluated temperatures (Supplementary Material - Table S2).

The GAB model was chosen to describe the water adsorption isotherms for the BSGs at all studied temperatures due to the advantage of having parameters with physical meaning. Figure 2 shows residual plot distributions for the GAB equation in all temperatures. A standard distribution in the residue's plots of the BSGs was verified. Residual values tend to increase with increasing water activity. Al-muhtaseb; Mcminn; Magee [25] considered GAB model as the most versatile model for predicting water adsorption isotherms of food-based products over a wide range of a_w.

Figure 2. Residual plot distributions for GAB equation in all temperatures.

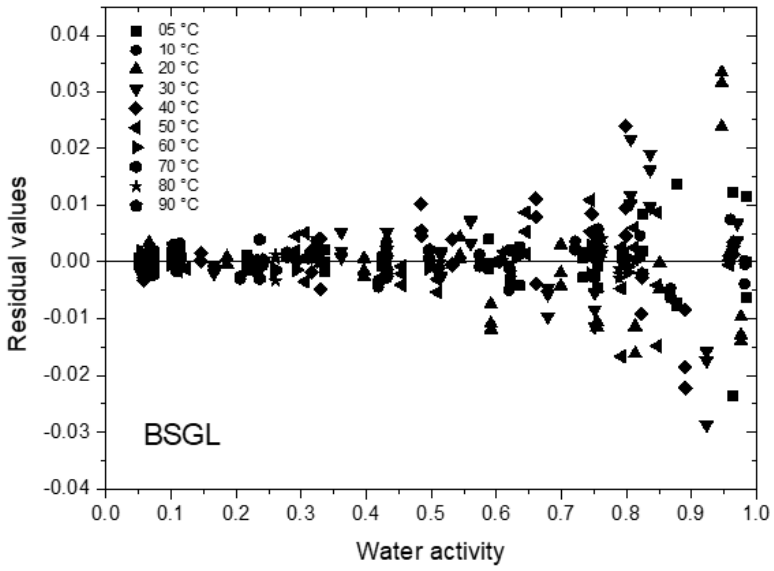

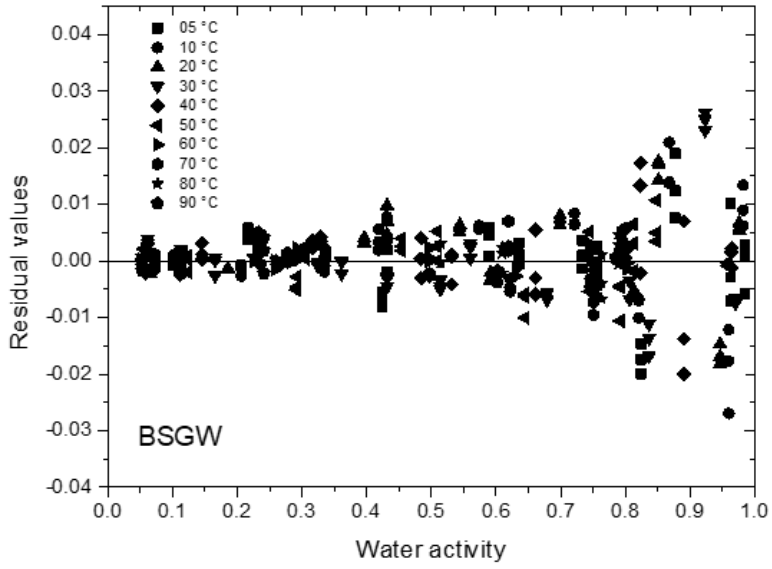

BSGL = Brewer's spent grain "Lager" style; BSGW = Brewer's spent grain "Weiss" style.

In fact, several studies concluded that GAB was the most suitable model to predict the isotherms of both food [52,53] and lignocellulosic-based materials [12,29,51]. The theoretical basis of the GAB model is the assumption of localized physical adsorption in multilayers with no lateral interactions: subsequent layers of water have less interaction with the sorbent surface and the first shell of water evenly covers the sorbent surface and is very tightly bound in a monolayer [54].

In the GAB model, the water content of the monolayer (X_m) corresponds to the amount of water strongly adsorbed to the primary adsorption sites. It is considered as the limit value of stability in foods because in this moisture range the rates of deterioration reactions due to the presence of water are negligible [14]. After the formation of the monolayer, water molecules occupy the adsorption sites to create the multilayers successively through relatively weak bonds [55].

Figure 3 shows the values of X_m as a function of temperature. The X_m values for BSGL and BSGW decreased because of the increase in temperature. The lowest values

of X_m were found for the isotherms at 90 °C and the highest values were found for the isotherms at 5 °C, corroborating the effects of temperature on the X_{eq} of the BSGs.

Figure 3. X_m values for BSGL and BSGW as a function of temperature.

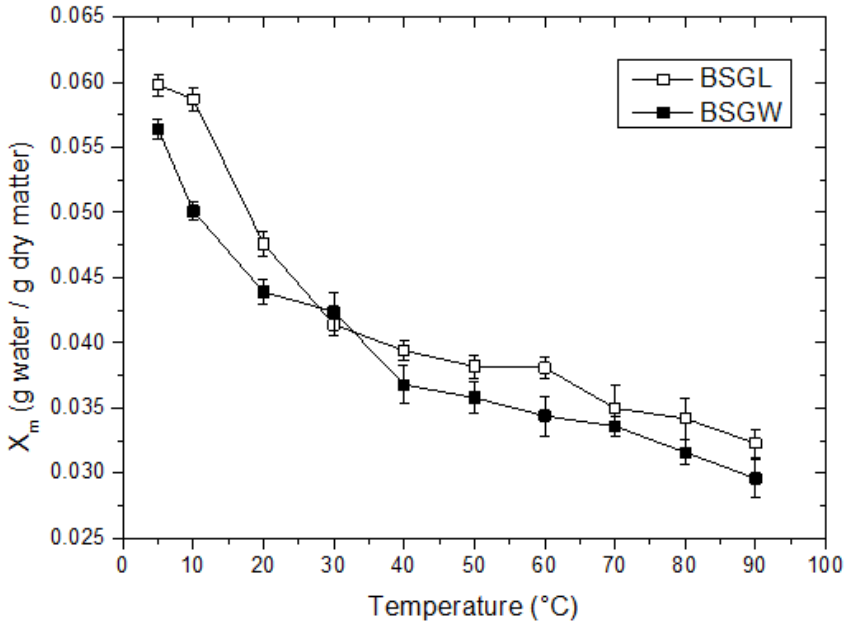

When analyzing the decay of the X_m values with increasing temperature, it could be seen that, above 40 ºC, such values had less significant decrease compared to lower temperatures. Together with the drying kinetics and energy consumption, this value can be considered when designing drying processes of BSGs to avoid spending energy without significant reduction in the monolayer moisture content.

The constant C is related to the binding strength of the monolayer's water to the matrix's active sites [56]. The increase in temperature caused a reduction in the values of C. This trend agrees with the decrease in X_m with increasing temperature, indicating that, above 40 ºC, there were not significant changes in the binding strength represented by C values. This decreasing behavior with increasing temperature has also been reported for other matrices such as non-conventional exudate gum (from *Prosopis alba*) [53] and tamarind seed mucilage [57]. Adsorbent-adsorbate interactions are likely exothermic, resulting in lower C values with increasing temperature [53,58].

The K values are related to the interactions between the adsorbent and the molecules in the multilayers. When K is equal to 1, the water in the multilayers has the properties of liquid water [59]. In this study, the K values were very close to the unit, ranging from 0.9372 to 0.9933 for all the samples and temperatures. Because the water molecules in the multilayers are weakly bound, behaving as liquid water, the need by subjecting the BSGs through adequate stabilization processes to limit the availability of free water for chemical reactions is reinforced. For this, the reported results become essential. Furthermore, the K values showed a tendency to increase as the temperature increased probably because of an increased agitation degree of the molecules by the temperature effect.

3.4 Adsorption surface area (ASA)

The ASA provides important information on the binding properties of water with the solid matrix [57]. This property was calculated using the parameter X_m obtained by the GAB model, through Equation (4) for the 10 temperatures evaluated in this study.

According to Figure 4, the results ranged from 114.01 to 211.09 $m^2 \cdot g^{-1}$ dry solids for BSGL and from 104.48 to 199.09 $m^2 \cdot g^{-1}$ dry solids for BSGW. The increase in temperature reduced the ASA for both BSGs, confirming that the availability of active sites and the binding energies associated with water sorption decreased, which probably caused the reduction in the total sorption capacity [60] of BSGs, corroborating the effects of temperature on water sorption isotherms (Figure 1). This reduction in the number of active sites is probably related to temperature-induced physical and chemical changes [16].

Figure 4. Adsorption surface area (ASA) of BSGs as a function of temperature (points are experimental data; vertical bars are the standard deviation).

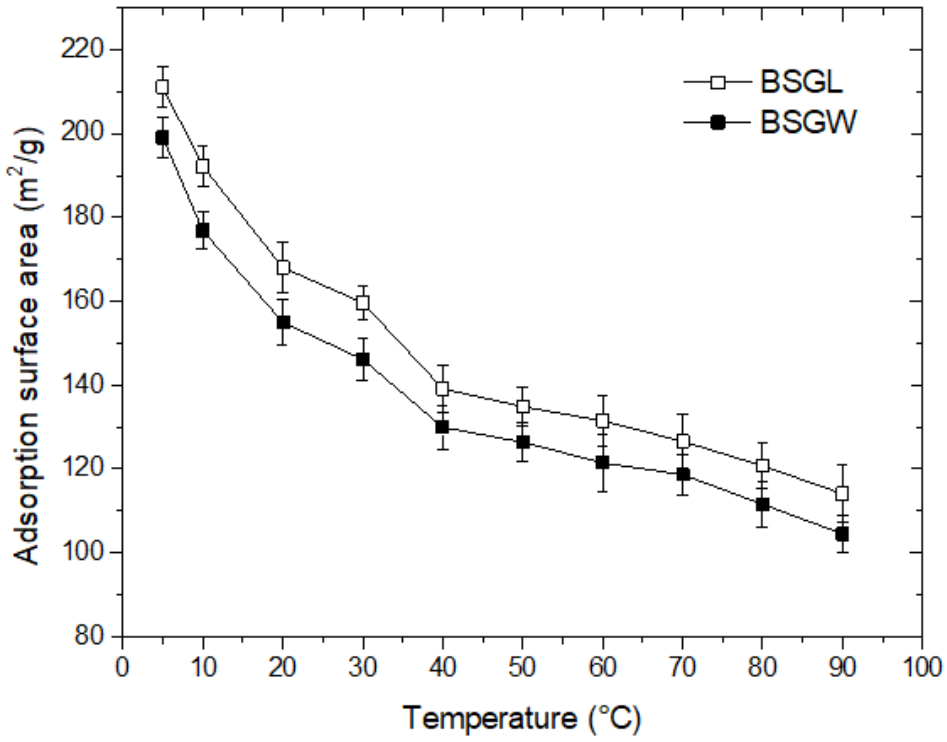

At low temperatures (up to 30 °C), BSGL showed a slightly higher ASA when compared to BSGW. The higher ASA in the BSGL may be related to the higher equilibrium moisture (X_{eq}) found in the isotherms of the BSGL (Figure 1), mainly in regions of water activity close to 1. The ASA of several agro-industrial by-products is due to the existence of an intrinsic microporous structure of these materials [13,57]. The number and size of pores, chemical composition, and the interaction of structure and surface in the matrix determine the total sorption area, while the surface pore properties influence the rate and extent of the sorption process [16,60] of the BSGs.

3.5 Spreading pressure (Φ)

The spreading pressure (Φ) can be understood as the driving force responsible for diffusion in porous solids [61], representing the excess free energy on the surface, showing the increase in surface tension at sorption sites due to absorbed molecules [62].

Figure 5 shows the spreading pressure as a function of water activity at different temperatures for the BSGL and for the BSGW.

Figure 5. Spreading pressure as a function of water activity at different temperatures for a) BSGL and b) BSGW (points are experimental data; vertical bars are the standard deviation).

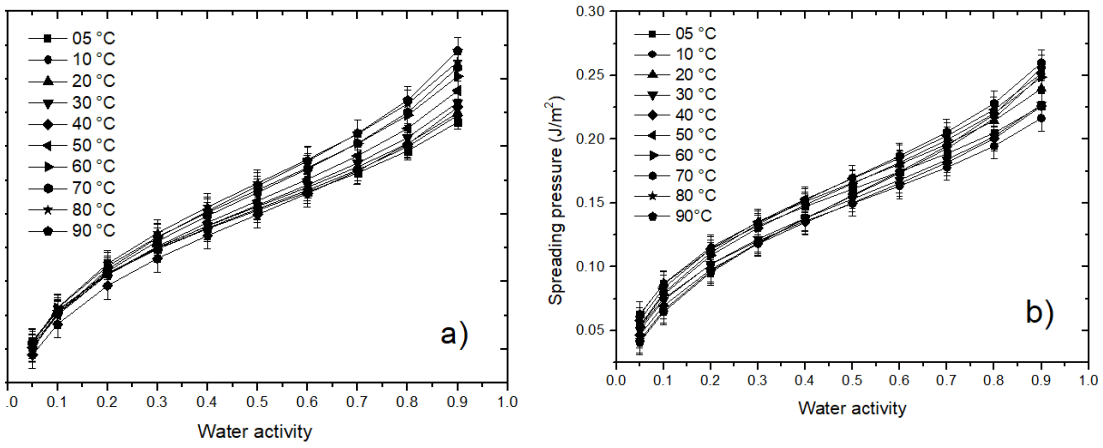

The results indicate that the Φ reduced mainly because of the reduction in the water activity of the BSGs. This shows that the reduction in water activity caused a reduction in the surface potential of the BSGs, reducing the free energy at the surface, which is the driving force responsible for diffusion. Higher spreading pressure values indicate a high affinity between active sites and water molecules. Thus, the higher the value of Φ, the more hygroscopic the product [61]. In contrast, there was a small effect of temperature on the values of Φ when compared to the effects of a_w. The Φ values decreased as the temperature decreased. This same behavior regarding temperature was reported in chestnut wood [29], potato and sweet potato flakes [62], and chironji kernels [63].

3.6 Thermodynamic properties

3.6.1 Net isosteric heat of adsorption (q_{st})

The net isosteric heat of adsorption (q_{st}) provides information on the state of water in foods and can also be used to estimate the amount of energy required during the drying

process [16] of BSGs. Given the satisfactory prediction of the water adsorption isotherms of the BSGs using the GAB model, the a_w predicted by this model at a constant equilibrium moisture content (X_{eq}), ranging from 0.1 to 0.45 g of water·g^{-1} dry matter, was used to determine the q_{st}.

According to Figure 6, the energy required for the water adsorption to occur varied from 140.88 to 12356.26 J·mol^{-1} for BSGL and from 156.71 to 14412,31 J·mol^{-1} for BSGW, in a range of X_{eq} between 0.05 and 0.45 (g water / g dry matter).

Figure 6. Net isosteric heat of sorption of BSGs as a function of equilibrium moisture content (points are experimental data; vertical bars are the standard deviation).

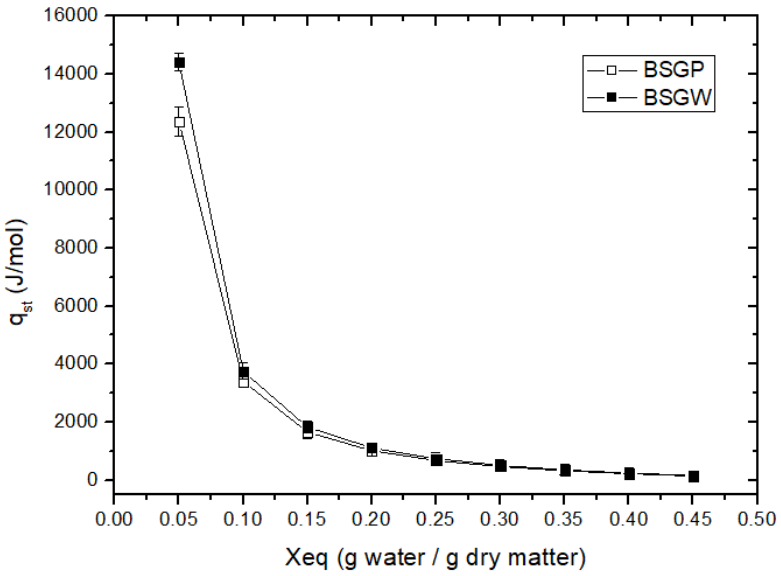

BSGL = Brewer's spent grain "Lager" style; BSGW = Brewer's spent grain "Weiss" style.

For cassava bagasse, Polachini et al. [12] reported q_{st} ranging between 850 and 21550 J/mol in a X_{eq} range from 0.05 up to 0.30 g water / g dry matter. Such values are similar in magnitude to the ones found in the present work. Rosa et al. [13] presented relatively lower q_{st} values for papaya seed, which ranged from 560 to 8710 J/mol in a X_{eq} interval between 0.30 and 0.48 g water / g dry matter. It is valid to highlight that such values depends on the equilibrium moisture content range investigated, but also on the studied material – reinforcing the need by studying each product specifically.

In both BSGs, an increase in q_{st} was observed due to the reduction of X_{eq}, showing that more heat is needed as the material's moisture decreases during drying. It can be related to the fact that, in regions of low moisture content, water molecules are strongly bound to macromolecules such as cellulose, hemicellulose, lignin, and proteins present in the structure of the material, when compared to water from adjacent multilayers. This trend was also observed in other lignocellulosic-based materials such as cassava bagasse [12], different types of wood [29] papaya seeds [13], and wheat malt [28].

As initially reported, the stability of this by-product is strongly dependent on a_w and X_{eq} conditions, which are key parameters for its management and use. In addition to the high a_w providing highly favorable conditions for the growth of microorganisms, non-enzymatic browning, and enzymatic reactions, it can also cause changes in the technological and sensory properties of this by-product when considering it as an ingredient in food products [64]. Thus, designing the ideal conditions for the water activity of the BSGs aiming at lower energy consumption during the drying process and maximum stability during storage can contribute to the management and reuse of BSGs with preserved quality.

Considering that microbial growth and enzymatic activity are the main responsible for drastically affecting the quality of BSGs, it is advisable to store such by-products under suitable conditions. According to Bonazzi; Dumoulin [61], these reactions have a high reaction rate above a water activity of 0.4. Another factor that can cause undesirable reactions is lipid oxidation, which has a lower reaction rate in water activity between 0.2 to 0.4. From an energy point of view, the lower the X_{eq}, the higher the enthalpy and heat of adsorption values, indicating that more energy is needed to remove water molecules under these conditions. Therefore, from an energy and stability point of view, the ideal long-term storage condition for BSGs was considered when the water

activity reached 0.4. Thus, BSGs must be stored in environments with a relative humidity of 40%, which can contribute to longer shelf life.

3.6.2 Differential enthalpy and entropy

Differential enthalpy and entropy are thermodynamic properties that can be used to evaluate the water adsorption behavior of BSGs. These properties were calculated using Equation (13), over a range of X_{eq} from 0.1 to 0.45 (dry basis). Enthalpy is a property that informs the variations of thermal energy involved between the water molecules with the matrix (sorbent) during the adsorption processes [66,67]. This property ranged from -3757.01 to -156.71 J·mol^{-1} for BSGL and from -3303.56 to -140.88 J·mol^{-1} for BSGW (Figure 7).

Figure 7. Change in enthalpy and entropy of BSGs as a function of equilibrium moisture contents (points are experimental data; vertical bars are the standard deviation).

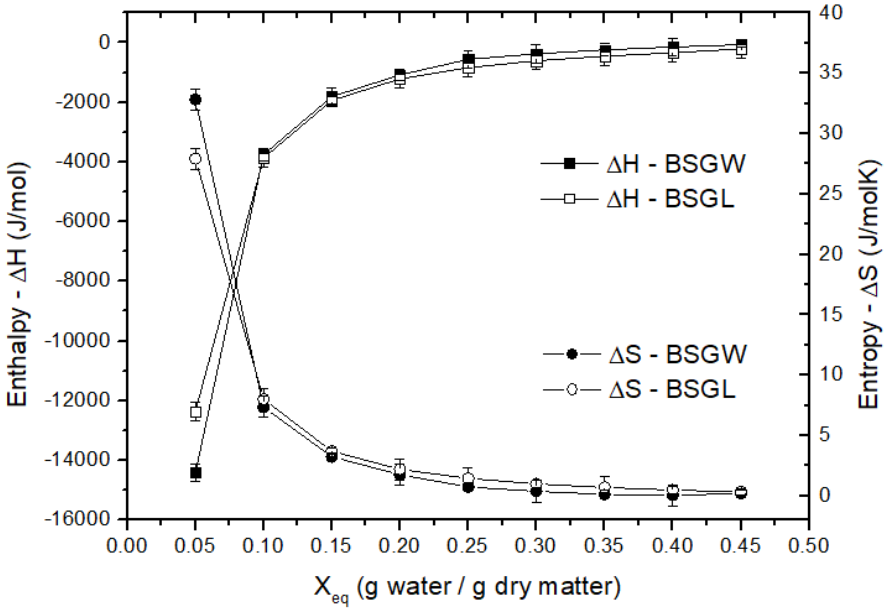

BSGL = Brewer's spent grain "Lager" style; BSGW = Brewer's spent grain "Weiss" style.

The negative enthalpy values indicates that there are binding forces involved in the adsorption process, in addition to characterizing the process as exothermic

[66,68]. Furthermore, this property is like the isosteric heat of adsorption, meaning it represents the energy required to do useful work [30].

Entropy is a measure of the degree of disorder in a water sorption system, being a measure of the unavailability of energy to carry out a given process [66], as in drying. In this study, the differential entropy ranged from 0.01 to 7.59 $J \cdot mol^{-1} \cdot K^{-1}$ for BSGL and from 0.003 to 6.60 $J \cdot mol^{-1} \cdot K^{-1}$ for BSGW (Figure 7). In modulus, both enthalpy and entropy increased as the moisture content of the BSGs is reduced. This is probably associated with reductions in adsorption surface area and spreading pressure (driving force responsible for diffusion in porous solids) as the material loses moisture, being this more expressive in regions with moisture below 0.2 g of water$\cdot g^{-1}$ of dry matter, indicating that more energy is needed to remove water molecules under these conditions. Furthermore, it is noteworthy that the moisture at which the maximum enthalpy and entropy values, in modulus, were reached are very close to the monolayer moisture values obtained from the GAB model. It is due to the presence of highly active polar sites that bind water to incorporate moisture in the food matrix monolayer [69]. On the other hand, the formation of multiple layers of adsorbed water is probably the main reason for the decrease in enthalpy and entropy with increasing moisture content [25]. The same behavior was reported in lignocellulosic materials such as cassava bagasse [12], papaya seeds [13],and different types of wood [29].

3.6.3 Enthalpy-entropy compensation theory

Compensation theory is used to evaluate physical and chemical phenomena [68], such as the water sorption reactions that occur during BSGs processing. Moreover, it provides information about the reaction mechanism and whether the reaction is controlled by enthalpy, where there will be greater molecular interaction due to the reduction of freedom or the binding of molecules in the system, generating greater organization or

order; or entropy, where there will be disorganization and greater freedom of molecules in the system [70].

Figure 8 presents the linear relationships between differential enthalpy and entropy for BSGs. These linear relationships are considered strong when the adjusted coefficients of determination (R^2_{adj}) were greater than 0.99, being the first important requirement to validate the existence of the theory of enthalpy-entropy compensation. In this work, it was found a R^2_{adj} higher than 0.999 for both samples, confirming that changes in entropy are linearly accompanied by changes in enthalpy.

Figure 8. Linear relationship between differential enthalpy and differential entropy values for BSGL and BSGW.

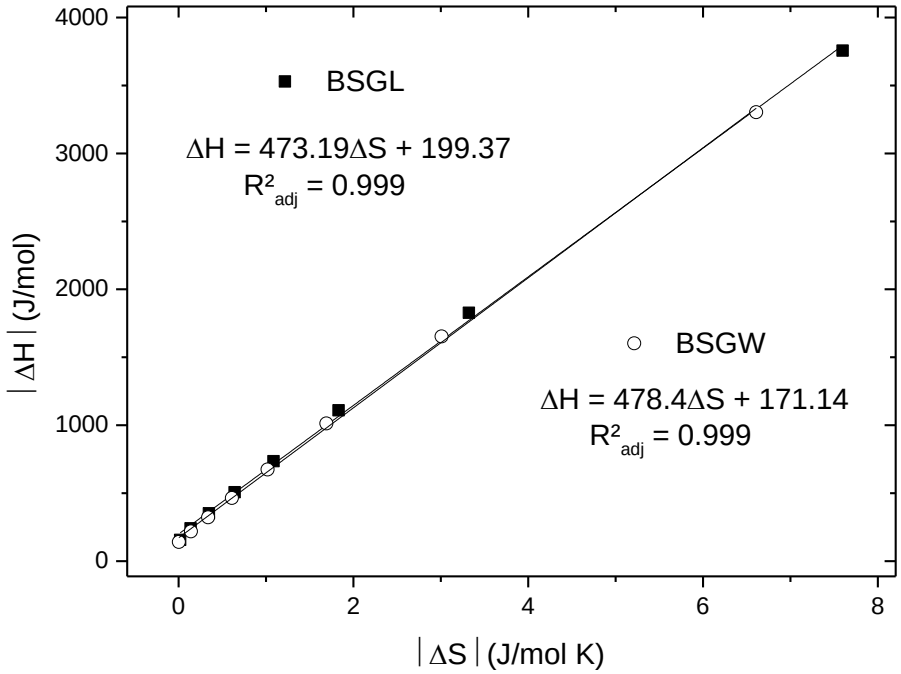

BSGL = Brewer's spent grain "Lager" style; BSGW = Brewer's spent grain "Weiss" style.

The second requirement to confirm the existence of the compensation theory is to compare the isokinetic temperature (T_b) with the harmonic mean temperature (T_{hm}). If these temperatures are statistically different, the second requirement to confirm a linear chemical compensation pattern is confirmed [31,32]. Therefore, the parameters T_b and ΔG_b were calculated using Equation (11).

The isokinetic temperature (T_b) for BSGL and BSGW were 473.19 ± 13.82 K and 478.4 ± 11.88 K, respectively. The harmonic mean temperature (T_{hm}) resulted in a value of 316.20 K for both BSGs. Thus, the harmonic mean temperature (T_{hm}) is significantly lower than the isokinetic temperature (T_b) with 95% confidence. This means that the adsorption process is enthalpy controlled [70]. In fact, the sorption of most products appears to be controlled by enthalpy [12,13,17]. Gabas; Menegalli; Telis-Romero [67] state that, when the water sorption process is controlled by enthalpy, the microstructure of the material is stable (within the studied temperature range) and does not significantly change during the water sorption phenomenon. The values of Gibbs free energy at the T_b (ΔG_b) obtained in the present study were 199.37 J·mol^{-1} for BSGL and 171.14 J·mol^{-1} for BSGW. Both assumed positive values, indicating that the adsorption process of BSGs is not spontaneous ($+\Delta G_b$). This fact may be related to the composition of BSGs in terms of lipids and proteins. Recently, Abeynayake et al. [36] studied BSG proteins and identified a high content of hydrophobic amino acid content of barley hordein and glutelins such as phenylalanine, valine, leucine, isoleucine, and methionine. These nonpolar components make the water adsorption phenomena difficult, corroborating the fact that the adsorption process is not spontaneous. This indicates that the product does not spontaneously absorb moisture from the environment, which is desirable for the stability of the by-product.

4 CONCLUSIONS

In this study, the water adsorption properties of brewer's spent grain (BSG) obtained from barley- and wheat-malt based brewery process (“Lager” – BSGL and “Weiss” – BSGW) were evaluated in a wide temperature range (5 - 90°C) to cover conditions for stabilization – from storage to drying processes. At temperatures from 5 to 50 °C, the adsorption isotherms of BSGL and BSGW showed convex curves, typical of type III isotherms. However, at temperatures above 60 °C, the curves started to present a

typical behavior of type II isotherms with sigmoid-shaped sorption. The equilibrium moisture increased as a result of the increase in relative humidity and reduction in temperature. Water binding properties seemed to be slightly hampered by the higher protein contents observed in BSGW samples. The GAB model was the most suitable model to describe the adsorption isotherms of BSGs, providing data on the monolayer moisture in this wide temperature range. Thermodynamic analysis showed that the net isosteric heat of adsorption and the differential entropy decreased as the equilibrium moisture increased. The spreading pressure increased mainly as the water activity increased. The linear relationship between enthalpy and entropy confirmed the theory of compensation and showed that the adsorption processes of BSGs were driven by enthalpy. The Gibbs free energy indicated that the adsorption processes were not spontaneous. From an energy and stability point of view, a water activity of 0.4 is the ideal condition for the storage of BSGs. Thus, this by-product must be stored in environments with a relative humidity of 40% to stabilize the BSGs, generating humidity levels between 0.05-0.09 (g of water·g^{-1} dry matter), depending on the temperature, which can contribute to longer shelf life for future applications in biorefinery and/or food applications.

Declaration of competing interest

The authors declare no conflict of interest.

Acknowledgments

This study was financed in part by the São Paulo Research Foundation (FAPESP) – Grant n°2022/05272-8 and by the Coordenação de Aperfeiçoamento de Pessoal de Nível Superior - Brasil (CAPES) - Finance Code 001.

This study was in part carried out in the Centre Européen de Biotechnologie et de Bioéconomie (CEBB), supported by the Région Grand Est, Département de la Marne, Greater Reims (France) and the European Union. In particular, the authors would like to thank the Département de la Marne, Greater Reims, Région Grand Est and the European Union along with the European Regional Development Fund (ERDF Champagne Ardenne 2014-2020) for their financial support of the Chair of Biotechnology of CentraleSupélec.

References

[1] M. Yang, X. Zhai, X. Huang, Z. Li, J. Shi, Q. Li, X. Zou, M. Battino, Rapid discrimination of beer based on quantitative aroma determination using colorimetric sensor array, Food Chem. 363 (2021) 130297. https://doi.org/10.1016/J.FOODCHEM.2021.130297.

[2] M. Kavalopoulos, V. Stoumpou, A. Christofi, S. Mai, E.M. Barampouti, K. Moustakas, D. Malamis, M. Loizidou, Sustainable valorisation pathways mitigating environmental pollution from brewers' spent grains, Environmental Pollution. 270 (2021) 116069. https://doi.org/10.1016/J.ENVPOL.2020.116069.

[3] N.P.P. Pabbathi, A. Velidandi, S. Pogula, P.K. Gandam, R.R. Baadhe, M. Sharma, R. Sirohi, V.K. Thakur, V.K. Gupta, Brewer's spent grains-based biorefineries: A critical review, Fuel. 317 (2022) 123435. https://doi.org/10.1016/J.FUEL.2022.123435.

[4] S.A.L. Bachmann, T. Calvete, L.A. Féris, Potential applications of brewery spent grain: Critical an overview, J Environ Chem Eng. 10 (2022) 106951. https://doi.org/10.1016/J.JECE.2021.106951.

[5] W. Li, H. Yang, T.E. Coldea, H. Zhao, Modification of structural and functional characteristics of brewer's spent grain protein by ultrasound assisted extraction, LWT. 139 (2021) 110582. https://doi.org/10.1016/J.LWT.2020.110582.

[6] R. Ibbett, R. White, G. Tucker, T. Foster, Hydro-mechanical processing of brewer's spent grain as a novel route for separation of protein products with differentiated techno-functional properties, Innovative Food Science & Emerging Technologies. 56 (2019) 102184. https://doi.org/10.1016/J.IFSET.2019.102184.

[7] T. Bonifácio-Lopes, A. Vilas-Boas, M. Machado, E.M. Costa, S. Silva, R.N. Pereira, D. Campos, J.A. Teixeira, M. Pintado, Exploring the bioactive potential

of brewers spent grain ohmic extracts, Innovative Food Science & Emerging Technologies. 76 (2022) 102943. https://doi.org/10.1016/J.IFSET.2022.102943.

[8] M. Panjičko, G.D. Zupančič, L. Fanedl, R.M. Logar, M. Tišma, B. Zelić, Biogas production from brewery spent grain as a mono-substrate in a two-stage process composed of solid-state anaerobic digestion and granular biomass reactors, J Clean Prod. 166 (2017) 519–529. https://doi.org/10.1016/J.JCLEPRO.2017.07.197.

[9] C. Moreirinha, C. Vilela, N.H.C.S. Silva, R.J.B. Pinto, A. Almeida, M.A.M. Rocha, E. Coelho, M.A. Coimbra, A.J.D. Silvestre, C.S.R. Freire, Antioxidant and antimicrobial films based on brewers spent grain arabinoxylans, nanocellulose and feruloylated compounds for active packaging, Food Hydrocoll. 108 (2020) 105836. https://doi.org/10.1016/J.FOODHYD.2020.105836.

[10] E. Wagner, M.E. Pería, G.E. Ortiz, N.L. Rojas, P.D. Ghiringhelli, Valorization of brewer's spent grain by different strategies of structural destabilization and enzymatic saccharification, Ind Crops Prod. 163 (2021) 113329. https://doi.org/10.1016/J.INDCROP.2021.113329.

[11] J. Naibaho, M. Korzeniowska, Brewers' spent grain in food systems: Processing and final products quality as a function of fiber modification treatment, J Food Sci. 86 (2021) 1532–1551. https://doi.org/10.1111/1750-3841.15714.

[12] T.C. Polachini, L.F.L. Betiol, J.F. Lopes-Filho, J. Telis-Romero, Water adsorption isotherms and thermodynamic properties of cassava bagasse, Thermochim Acta. 632 (2016) 79–85. https://doi.org/10.1016/j.tca.2016.03.032.

[13] D.P. Rosa, R.R. Evangelista, A.L. Borges Machado, M.A.R. Sanches, J. Telis-Romero, Water sorption properties of papaya seeds (Carica papaya L.) formosa variety: An assessment under storage and drying conditions, LWT. 138 (2021) 110458. https://doi.org/10.1016/j.lwt.2020.110458.

[14] M.L.F. Freitas, T.C. Polachini, A.C. de Souza, J. Telis-Romero, Sorption isotherms and thermodynamic properties of grated Parmesan cheese, Int J Food Sci Technol. 51 (2016) 250–259. https://doi.org/10.1111/ijfs.12969.

[15] R. Moreira, F. Chenlo, M.D. Torres, N. Vallejo, Thermodynamic analysis of experimental sorption isotherms of loquat and quince fruits, J Food Eng. 88 (2008) 514–521. https://doi.org/10.1016/J.JFOODENG.2008.03.011.

[16] B.K. Koua, P.M.E. Koffi, P. Gbaha, S. Toure, Thermodynamic analysis of sorption isotherms of cassava (Manihot esculenta), J Food Sci Technol. 51 (2014) 1711–1723. https://doi.org/10.1007/s13197-012-0687-y.

[17] C. Carvalho Lago, C.P.Z. Noreña, Thermodynamic analysis of sorption isotherms of dehydrated yacon (Smallanthus sonchifolius) bagasse, Food Biosci. 12 (2015) 26–33. https://doi.org/10.1016/J.FBIO.2015.07.001.

[18] MAPA. Ministério da Agricultura, Pecuária e Abastecimento. Instrução normativa nº 65, de 10 de dezembro de 2019. Estabelece os padrões de identidade e qualidade para os produtos de cervejaria. Diário Oficial da União: seção 1, Brasília, DF, ed. 239, p. 31.

[19] AOAC, Association of Official Analytical Chemistry, 18th ed., Gaithersburg, 2007.

[20] A. Sluiter, R. Ruiz, C. Scarlata, J. Sluiter & D. J. Templeton, Determination of extractives in biomass. Laboratory analytical procedure (LAP) 1617.4 (2008) 1-16.

[21] A. Sluiter, R. Ruiz, C. Scarlata, J. Sluiter & D. J. Determination of structural carbohydrates and lignin in biomass. Laboratory analytical procedure (LAP) 1617.1 (2008): 1-16.

[22] J. L. Gomide and J. D. Braz. Determinação do teor de lignina em material lenhoso: método Klason modificado. O papel 47 (1986) 36-38.

[23] Goldschimid, O. Ultraviolet spectra. Lignins: occurrence, formation, structure and reactions 1 (1971) 241-266.

[24] K. Filippi, H. Papapostolou, M. Alexandri, A. Vlysidis, E.D. Myrtsi, D. Ladakis, C. Pateraki, S.A. Haroutounian, A. Koutinas, Integrated biorefinery development using winery waste streams for the production of bacterial cellulose, succinic acid and value-added fractions, Bioresour Technol. 343 (2022) 125989. https://doi.org/10.1016/J.BIORTECH.2021.125989.

[25] A.H. Al-Muhtaseb, W.A.M. McMinn, T.R.A. Magee, Moisture Sorption Isotherm Characteristics of Food Products: A Review, Food and Bioproducts Processing. 80 (2002) 118–128. https://doi.org/10.1205/09603080252938753.

[26] T. Labuza, Creation of moisture sorption isotherms for hygroscopic materials. Sorption isotherm methods. In International Symposium on Humidity and Moisture. (1963). Washington: American Society of Heating, Refrigerating and Air Conditioning Engineers.

[27] R. Martínez-Las Heras, A. Heredia, M.L. Castelló, A. Andrés, Moisture sorption isotherms and isosteric heat of sorption of dry persimmon leaves, Food Biosci. 7 (2014) 88–94. https://doi.org/10.1016/J.FBIO.2014.06.002.

[28] K.S. Silva, T.C. Polachini, M. Luna-Flores, G. Luna-Solano, O. Resende, J. Telis-Romero, Sorption isotherms and thermodynamic properties of wheat malt under storage conditions, J Food Process Eng. (2021) e13784. https://doi.org/10.1111/jfpe.13784.

[29] C. Simón, L.G. Esteban, P. de Palacios, F.G. Fernández, A. García-Iruela, Thermodynamic properties of the water sorption isotherms of wood of limba (Terminalia superba Engl. & Diels), obeche (Triplochiton scleroxylon K. Schum.), radiata pine (Pinus radiata D. Don) and chestnut (Castanea sativa Mill.), Ind Crops Prod. 94 (2016) 122–131. https://doi.org/10.1016/J.INDCROP.2016.08.008.

[30] S.S.H. Rizvi, Thermodynamic Properties of Foods in Dehydration, in: M.A. Rao, S.S.H. Rizvi, A.K. Datta (Eds.), Engineering Properties of Foods, 3rd ed., Taylor & Francis Group, Boca Raton, FL, 2005.

[31] R.R. Krug, W.G. Hunter, R.A. Grieger, Enthalpy-entropy compensation. 1. Some fundamental statistical problems associated with the analysis of van't hoff and arrhenius data, Journal of Physical Chemistry. 80 (1976) 2335–2341. https://doi.org/10.1021/j100562a006.

[32] R.R. Krug, W.G. Hunter, R.A. Grieger, Enthalpy-entropy compensation. 2. Separation of the chemical from the statistical effect, Journal of Physical Chemistry. 80 (1976) 2341–2351. https://doi.org/10.1021/j100562a007.

[33] Z.X. Lu, J.F. He, Y.C. Zhang, D.J. Bing, Composition, physicochemical properties of pea protein and its application in functional foods, Https://Doi.Org/10.1080/10408398.2019.1651248. 60 (2019) 2593–2605. https://doi.org/10.1080/10408398.2019.1651248.

[34] P. Mattila, S. Mäkinen, M. Eurola, T. Jalava, J.M. Pihlava, J. Hellström, A. Pihlanto, Nutritional Value of Commercial Protein-Rich Plant Products, Plant Foods for Human Nutrition. 73 (2018) 108–115. https://doi.org/10.1007/S11130-018-0660-7/TABLES/4.

[35] F.G.B. Los, A.A.F. Zielinski, J.P. Wojeicchowski, A. Nogueira, I.M. Demiate, Beans (Phaseolus vulgaris L.): whole seeds with complex chemical composition, Curr Opin Food Sci. 19 (2018) 63–71. https://doi.org/10.1016/J.COFS.2018.01.010.

[36] R. Abeynayake, S. Zhang, W. Yang, L. Chen, Development of antioxidant peptides from brewers' spent grain proteins, LWT. 158 (2022) 113162. https://doi.org/10.1016/J.LWT.2022.113162.

[37] M. Tan, M.A. Nawaz, R. Buckow, Functional and food application of plant proteins – a review, Https://Doi.Org/10.1080/87559129.2021.1955918. (2021). https://doi.org/10.1080/87559129.2021.1955918.

[38] A.G.A. Sá, Y.M.F. Moreno, B.A.M. Carciofi, Plant proteins as high-quality nutritional source for human diet, Trends Food Sci Technol. 97 (2020) 170–184. https://doi.org/10.1016/J.TIFS.2020.01.011.

[39] W.G. Sganzerla, G.L. Zabot, P.C. Torres-Mayanga, L.S. Buller, S.I. Mussatto, T. Forster-Carneiro, Techno-economic assessment of subcritical water hydrolysis process for sugars production from brewer's spent grains, Ind Crops Prod. 171 (2021) 113836. https://doi.org/10.1016/J.INDCROP.2021.113836.

[40] M.A. Ribeiro Sanches, C. Camelo-Silva, L. Tussolini, M. Tussolini, R.C. Zambiazi, P. Becker Pertuzatti, Development, characterization and optimization of biopolymers films based on starch and flour from jabuticaba (Myrciaria cauliflora) peel, Food Chem. 343 (2021) 128430. https://doi.org/10.1016/j.foodchem.2020.128430.

[41] M.A. Ribeiro Sanches, C. Camelo-Silva, C. da Silva Carvalho, J. Rafael de Mello, N.G. Barroso, E. Lopes da Silva Barros, P.P. Silva, P.B. Pertuzatti, Active packaging with starch, red cabbage extract and sweet whey: Characterization and application in meat, LWT. 135 (2021) 110275. https://doi.org/10.1016/j.lwt.2020.110275.

[42] G.K. Shroti, C.S. Saini, Development of edible films from protein of brewer's spent grain: Effect of pH and protein concentration on physical, mechanical and barrier properties of films, Applied Food Research. 2 (2022) 100043. https://doi.org/10.1016/J.AFRES.2022.100043.

[43] A. Revert, M. Reig, V.J. Seguí, T. Boronat, V. Fombuena, R. Balart, Upgrading brewer's spent grain as functional filler in polypropylene matrix, Polym Compos. 38 (2017) 40–47. https://doi.org/10.1002/PC.23558.

[44] J. Weiermüller, A. Akermann, W. Laudensack, J. Chodorski, L.M. Blank, R. Ulber, Brewers' spent grain as carbon source for itaconate production with engineered Ustilago maydis, Bioresour Technol. 336 (2021) 125262. https://doi.org/10.1016/J.BIORTECH.2021.125262.

[45] A. Akermann, J. Weiermüller, J. Christmann, L. Guirande, G. Glaser, A. Knaus, R. Ulber, Brewers' spent grain liquor as a feedstock for lactate production with Lactobacillus delbrueckii subsp. lactis, Eng Life Sci. 20 (2020) 168–180. https://doi.org/10.1002/ELSC.201900143.

[46] J.C. López-Linares, M.T. García-Cubero, S. Lucas, M. Coca, Integral valorization of cellulosic and hemicellulosic sugars for biobutanol production: ABE fermentation of the whole slurry from microwave pretreated brewer's spent grain, Biomass Bioenergy. 135 (2020) 105524. https://doi.org/10.1016/J.BIOMBIOE.2020.105524.

[47] S. Brunauer, L.S. Deming, W.E. Deming, E. Teller, On the theory of the van der Waals adsorption of gases, J Am Chem Soc. 62 (1940) 1723–1732.

[48] M. Mathlouthi, Water content, water activity, water structure and the stability of foodstuffs, Food Control. 12 (2001) 409–417. https://doi.org/10.1016/S0956-7135(01)00032-9.

[49] N. Singh, J. Singh, L. Kaur, N.S. Sodhi, B.S. Gill, Morphological, thermal and rheological properties of starches from different botanical sources, Food Chem. 81 (2003) 219–231. https://doi.org/10.1016/S0308-8146(02)00416-8.

[50] M.A. Lazouk, R. Savoire, A. Kaddour, J. Castello, J.L. Lanoisellé, E. Van Hecke, B. Thomasset, Oilseeds sorption isoterms, mechanical properties and pressing: Global view of water impact, J Food Eng. 153 (2015) 73–80. https://doi.org/10.1016/j.jfoodeng.2014.12.008.

[51] Q. Chen, G. Wang, X.X. Ma, M.L. Chen, C.H. Fang, B.H. Fei, The effect of graded fibrous structure of bamboo (Phyllostachys edulis) on its water vapor sorption isotherms, Ind Crops Prod. 151 (2020) 112467. https://doi.org/10.1016/J.INDCROP.2020.112467.

[52] L.F.L. Betiol, R.R. Evangelista, M.A.R. Sanches, R.C. Basso, B. Gullón, J.M. Lorenzo, A.C. da S. Barretto, J. Telis-Romero, Influence of temperature and chemical composition on water sorption isotherms for dry-cured ham, Lwt. 123 (2020) 109112. https://doi.org/10.1016/j.lwt.2020.109112.

[53] F.E. Vasile, M.A. Judis, M.F. Mazzobre, Moisture sorption properties and glass transition temperature of a non-conventional exudate gum (Prosopis alba) from

northeast Argentine, Food Research International. 131 (2020) 109033. https://doi.org/10.1016/J.FOODRES.2020.109033.

[54] E.J. Quirijns, A.J.B. van Boxtel, W.K.P. van Loon, G. van Straten, Sorption isotherms, GAB parameters and isosteric heat of sorption, J Sci Food Agric. 85 (2005) 1805–1814. https://doi.org/10.1002/JSFA.2140.

[55] S. Kaya, T. Kahyaoglu, Thermodynamic properties and sorption equilibrium of pestil (grape leather), J Food Eng. 71 (2005) 200–207. https://doi.org/10.1016/J.JFOODENG.2004.10.034.

[56] K. Muzaffar, P. Kumar, Moisture sorption isotherms and storage study of spray dried tamarind pulp powder, Powder Technol. 291 (2016) 322–327. https://doi.org/10.1016/J.POWTEC.2015.12.046.

[57] E. Alpizar-Reyes, H. Carrillo-Navas, R. Romero-Romero, V. Varela-Guerrero, J. Alvarez-Ramírez, C. Pérez-Alonso, Thermodynamic sorption properties and glass transition temperature of tamarind seed mucilage (Tamarindus indica L.), Food and Bioproducts Processing. 101 (2017) 166–176. https://doi.org/10.1016/J.FBP.2016.11.006.

[58] L.L. Diosady, S.S.H. Rizvi, W. Cai, D.J. Jagdeo, Moisture Sorption Isotherms of Canola Meals, and Applications to Packaging, J Food Sci. 61 (1996) 204–208. https://doi.org/10.1111/J.1365-2621.1996.TB14760.X.

[59] C. Pérez-Alonso, C.I. Beristain, C. Lobato-Calleros, M.E. Rodríguez-Huezo, E.J. Vernon-Carter, Thermodynamic analysis of the sorption isotherms of pure and blended carbohydrate polymers, J Food Eng. 77 (2006) 753–760. https://doi.org/10.1016/J.JFOODENG.2005.08.002.

[60] S.K. Velázquez-Gutiérrez, A.C. Figueira, M.E. Rodríguez-Huezo, A. Román-Guerrero, H. Carrillo-Navas, C. Pérez-Alonso, Sorption isotherms, thermodynamic properties and glass transition temperature of mucilage extracted from chia seeds (Salvia hispanica L.), Carbohydr Polym. 121 (2015) 411–419. https://doi.org/10.1016/j.carbpol.2014.11.068.

[61] M.D. Torres, R. Moreira, F. Chenlo, M.J. Vázquez, Water adsorption isotherms of carboxymethyl cellulose, guar, locust bean, tragacanth and xanthan gums, Carbohydr Polym. 89 (2012) 592–598. https://doi.org/10.1016/J.CARBPOL.2012.03.055.

[62] C.C. Lago, M. Liendo-Cárdenas, C.P.Z. Noreña, Thermodynamic sorption properties of potato and sweet potato flakes, Food and Bioproducts Processing. 91 (2013) 389–395. https://doi.org/10.1016/J.FBP.2013.02.005.

[63] S.N. Sahu, A. Tiwari, J.K. Sahu, S.N. Naik, I. Baitharu, E. Kariali, Moisture sorption isotherms and thermodynamic properties of sorbed water of chironji (Buchanania lanzan Spreng.) kernels at different storage conditions, Journal of Food Measurement and Characterization. 12 (2018) 2626–2635. https://doi.org/10.1007/S11694-018-9880-7/TABLES/3.

[64] J. Naibaho, N. Butula, E. Jonuzi, M. Korzeniowska, O. Laaksonen, M. Föste, M.L. Kütt, B. Yang, Potential of brewers' spent grain in yogurt fermentation and

evaluation of its impact in rheological behaviour, consistency, microstructural properties and acidity profile during the refrigerated storage, Food Hydrocoll. 125 (2022) 107412. https://doi.org/10.1016/J.FOODHYD.2021.107412.

[65] C. Bonazzi, E. Dumoulin, Quality Changes in Food Materials as Influenced by Drying Processes, Modern Drying Technology. (2014) 1–20. https://doi.org/10.1002/9783527631728.CH14.

[66] W.A.M. McMinn, A.H. Al-Muhtaseb, T.R.A. Magee, Enthalpy–entropy compensation in sorption phenomena of starch materials, Food Research International. 38 (2005) 505–510. https://doi.org/10.1016/J.FOODRES.2004.11.004.

[67] A. Garvín, P.E.D. Augusto, R. Ibarz, A. Ibarz, Kinetic and thermodynamic compensation study of the hydration of faba beans (Vicia faba L.), Food Research International. 119 (2019) 390–397. https://doi.org/10.1016/J.FOODRES.2019.02.002.

[68] A. Garvín, R. Ibarz, A. Ibarz, Kinetic and thermodynamic compensation. A current and practical review for foods, Food Research International. 96 (2017) 132–153. https://doi.org/10.1016/J.FOODRES.2017.03.004.

[69] M.A. Al-Mahasneh, M.M. Bani Amer, T.M. Rababah, Modeling moisture sorption isotherms in roasted green wheat using least square regression and neural-fuzzy techniques, Food and Bioproducts Processing. 90 (2012) 165–170. https://doi.org/10.1016/J.FBP.2011.02.007.

[70] J.C. Spada, C.P.Z. Noreña, L.D.F. Marczak, I.C. Tessaro, Water adsorption isotherms of microcapsules with hydrolyzed pinhão (Araucaria angustifolia seeds) starch as wall material, J Food Eng. 114 (2013) 64–69. https://doi.org/10.1016/j.jfoodeng.2012.07.019.

[71] A.L. Gabas, F.C. Menegalli, J. Telis-Romero, Water Sorption Enthalpy-Entropy Compensation Based on Isotherms of Plum Skin and Pulp, J Food Sci. 65 (2000) 680–680. https://doi.org/10.1111/J.1365-2621.2000.TB16072.X.

Nomenclature

$(NH_4)_2SO_4$ - Ammonium Sulfate

ΔG - Gibbs free energy

ΔGB - Free Gibbs energy at isokinetic temperature

ΔH - Differential enthalpy of sorption

ΔS - Differential entropy of sorption

A_m - Surface area of a water molecule

A_{H2O} - Area of a water molecule

ASA - Adsorption surface area

a_w - Water activity

BSG - Brewer's spent grain

BSGL - Brewer's spent grain "Lager" style

BSGW - Brewer's spent grain "Weiss" style

db - Dry basis

ELSD - Evaporative light scattering detector

GAB – GAB model

HPLC - High-performance liquid chromatography

h_1 and h_2 - Constants of Halsey model

H_1 and H_2 - Constants of Henderson model

k_1, k_2, n_1 and n_2 - Constants of Peleg model

K_2CO_3 - Potassium carbonate

K_2SO_4 - Potassium Sulfate

K_B - Boltzmann constant

KCl - Potassium chloride

KI - Potassium iodide

KNO_3 - Potassium Nitrate

LiBr - Lithium bromide

LiCl - Lithium chloride

M and N - Constants of Oswin model

$Mg(NO_3)_2$ - Magnesium nitrate

$MgCl_2$ - Magnesium chloride

M_{H2O} - Molecular weight of water

NaBr - Sodium bromide

NaCl - Sodium chloride

NaI - Sodium iodide

q_{st} - Net isosteric heat of sorption

RHs - Relative humidities

R - Universal gas constant

R^2_{Adj} - Adjusted determination coefficients

T - Absolute temperature (K)

T_B - Isokinetic temperature

T_{hm} - Harmonic mean temperature

X_{eq} - Equilibrium moisture content

X_m - Monolayer moisture content

X_m, C and K - Constant of GAB model

λ - Heat vaporization of pure water

Φ - Spreading pressure

χ^2 - Chi-square

Appendix A. Supplementary data

Table S1. Experimental data on equilibrium moisture content of BSGs versus water activity at the temperatures studied (average ± standard deviation).

5 °C			10 °C			20 °C			30 °C		
a_w*	X_{eq}		a_w*	X_{eq}		a_w*	X_{eq}		a_w*	X_{eq}	
	BSGL	BSGW		BSGL	BSGW		BSGL	BSGW		BSGL	BSGW
0.0743	0.0473 ± 0.0008	0.0400 ± 0.0019	0.0714	0.0407 ± 0.0005	0.0430 ± 0.0003	0.0661	0.0487 ± 0.0009	0.0348 ± 0.0008	0.0616	0.0343 ± 0.0006	0.0323 ± 0.0015
0.1126	0.0544 ± 0.0008	0.0462 ± 0.0019	0.1129	0.0481 ± 0.0003	0.0482 ± 0.0011	0.1131	0.0577 ± 0.0014	0.0410 ± 0.0006	0.1128	0.0411 ± 0.0006	0.0385 ± 0.0014
0.2168	0.0668 ± 0.0018	0.0662 ± 0.0030	0.2061	0.0554 ± 0.0006	0.0568 ± 0.0012	0.1856	0.0622 ± 0.0016	0.0477 ± 0.0006	0.1657	0.0445 ± 0.0011	0.0419 ± 0.0011
0.3360	0.0814 ± 0.0012	0.0775 ± 0.0027	0.3347	0.0710 ± 0.0005	0.0700 ± 0.0003	0.3307	0.0785 ± 0.0016	0.0615 ± 0.0009	0.3244	0.0608 ± 0.0013	0.0564 ± 0.0004
0.4242	0.0938 ± 0.0018	0.0818 ± 0.0020	0.4183	0.0780 ± 0.0010	0.0843 ± 0.0017	0.3965	0.0860 ± 0.0018	0.0724 ± 0.0009	0.3615	0.0645 ± 0.0029	0.0599 ± 0.0017
0.4313	0.0958 ± 0.0022	0.0911 ± 0.0014	0.4314	0.0829 ± 0.0011	0.0899 ± 0.0016	0.4316	0.0925 ± 0.0025	0.0803 ± 0.0022	0.4317	0.0721 ± 0.0028	0.0650 ± 0.0002
0.5886	0.1293 ± 0.0011	0.1259 ± 0.0018	0.5736	0.1065 ± 0.0022	0.1134 ± 0.0020	0.5438	0.1201 ± 0.0017	0.0963 ± 0.0006	0.5140	0.0808 ± 0.0019	0.0757 ± 0.0012
0.6351	0.1426 ± 0.0030	0.1372 ± 0.0058	0.6215	0.1058 ± 0.0037	0.1149 ± 0.0035	0.5914	0.1301 ± 0.0026	0.0975 ± 0.0013	0.5603	0.0947 ± 0.0017	0.0901 ± 0.0005
0.7330	0.1854 ± 0.0017	0.1783 ± 0.0038	0.7211	0.1520 ± 0.0022	0.1618 ± 0.0034	0.6990	0.1746 ± 0.0037	0.1402 ± 0.0009	0.6789	0.1119 ± 0.0028	0.1114 ± 0.0019
0.7565	0.1995 ± 0.0029	0.1910 ± 0.0077	0.7567	0.1738 ± 0.0029	0.1671 ± 0.0035	0.7547	0.1949 ± 0.0066	0.1552 ± 0.0027	0.7509	0.1399 ± 0.0019	0.1442 ± 0.0026
0.8242	0.2590 ± 0.0070	0.2279 ± 0.0070	0.8206	0.2161 ± 0.0047	0.2110 ± 0.0025	0.8134	0.2447 ± 0.0043	0.1953 ± 0.0029	0.8063	0.1984 ± 0.0070	0.1772 ± 0.0061
0.8767	0.3273 ± 0.0132	0.3268 ± 0.0062	0.8677	0.2703 ± 0.0017	0.2884 ± 0.0024	0.8511	0.2951 ± 0.0069	0.2582 ± 0.0043	0.8362	0.2260 ± 0.0057	0.1912 ± 0.0026
0.9627	0.5972 ± 0.0186	0.5749 ± 0.0205	0.9596	0.5613 ± 0.0054	0.4971 ± 0.0107	0.9462	0.5675 ± 0.0192	0.4747 ± 0.0084	0.9231	0.3486 ± 0.0094	0.3698 ± 0.0030
0.9848	0.7648 ± 0.0155	0.7294 ± 0.0098	0.9818	0.7403 ± 0.0073	0.6677 ± 0.0039	0.9759	0.7143 ± 0.0187	0.7295 ± 0.0149	0.9700	0.6236 ± 0.0109	0.5370 ± 0.0091

40 °C			50 °C			60 °C			70 °C		
a_w*	X_{eq}		a_w*	X_{eq}		a_w*	X_{eq}		a_w*	X_{eq}	
	BSGL	BSGW		BSGL	BSGW		BSGL	BSGW		BSGL	BSGW
0.0580	0.0315 ± 0.0006	0.0305 ± 0.0004	0.0553	0.0307 ± 0.0016	0.0281 ± 0.0019	0.0533	0.0289 ± 0.0009	0.0275 ± 0.0019	0.0523	0.0269 ± 0.0020	0.0236 ± 0.0011
0.1121	0.0400 ± 0.0006	0.0343 ± 0.0003	0.1110	0.0374 ± 0.0029	0.0350 ± 0.0018	0.1095	0.0362 ± 0.0006	0.0339 ± 0.0014	0.1075	0.0325 ± 0.0012	0.0297 ± 0.0002
0.1455	0.0431 ± 0.0008	0.0402 ± 0.0012	0.1238	0.0372 ± 0.0011	0.0354 ± 0.0025	0.0998	0.0358 ± 0.0009	0.0328 ± 0.0017	0.0723	0.0304 ± 0.0015	0.0263 ± 0.0011
0.3160	0.0554 ± 0.0021	0.0531 ± 0.0009	0.3054	0.0527 ± 0.0031	0.0509 ± 0.0004	0.2926	0.0500 ± 0.0010	0.0472 ± 0.0021	0.2777	0.0470 ± 0.0003	0.0415 ± 0.0005
0.3288	0.0565 ± 0.0043	0.0547 ± 0.0009	0.2921	0.0532 ± 0.0012	0.0441 ± 0.0019	0.2595	0.0463 ± 0.0015	0.0429 ± 0.0018	0.2357	0.0429 ± 0.0036	0.0410 ± 0.0025
0.4842	0.0798 ± 0.0036	0.0668 ± 0.0019	0.4544	0.0643 ± 0.0032	0.0663 ± 0.0008	0.4966	0.0709 ± 0.0032	0.0672 ± 0.0027	0.4970	0.0689 ± 0.0002	0.0590 ± 0.0008
0.5317	0.0811 ± 0.0032	0.0720 ± 0.0046	0.5093	0.0705 ± 0.0005	0.0732 ± 0.0019	0.6311	0.0974 ± 0.0036	0.0871 ± 0.0023	0.6193	0.0874 ± 0.0051	0.0837 ± 0.0041
0.6609	0.1134 ± 0.0070	0.0973 ± 0.0042	0.6449	0.1053 ± 0.0018	0.0883 ± 0.0030	0.7450	0.1352 ± 0.0080	0.1261 ± 0.0009	0.7506	0.1321 ± 0.0018	0.1137 ± 0.0028
0.7468	0.1462 ± 0.0032	0.1263 ± 0.0031	0.7443	0.1408 ± 0.0069	0.1287 ± 0.0060	0.8025	0.1672 ± 0.0057	0.1593 ± 0.0088	0.7949	0.1619 ± 0.0059	0.1486 ± 0.0036
0.7991	0.1852 ± 0.0091	0.1588 ± 0.0033	0.7920	0.1550 ± 0.0073	0.1472 ± 0.0041						
0.8232	0.1877 ± 0.0052	0.1845 ± 0.0086	0.8120	0.1788 ± 0.0013	0.1700 ± 0.0037						
0.8903	0.2660 ± 0.0104	0.2481 ± 0.0125	0.8478	0.2060 ± 0.0140	0.2054 ± 0.0035						
0.9641	0.5823 ± 0.0108	0.5317 ± 0.0353	0.9582	0.5074 ± 0.0081	0.4712 ± 0.0056						

80 °C			90 °C		
a_w*	X_{eq}		a_w*	X_{eq}	
	BSGL	BSGW		BSGL	BSGW
0.0520	0.0248 ± 0.0008	0.0250 ± 0.0004	0.0526	0.0243 ± 0.0003	0.0253 ± 0.0023
0.1051	0.0317 ± 0.0008	0.0307 ± 0.0003	0.1023	0.0311 ± 0.0011	0.0301 ± 0.0018
0.2605	0.0421 ± 0.0012	0.0416 ± 0.0008	0.2412	0.0386 ± 0.0006	0.0390 ± 0.0005
0.2252	0.0400 ± 0.0015	0.0399 ± 0.0006	0.2325	0.0372 ± 0.0020	0.0400 ± 0.0056
0.5143	0.0652 ± 0.0037	0.0651 ± 0.0032	0.6021	0.0804 ± 0.0061	0.0703 ± 0.0062
0.6097	0.0825 ± 0.0044	0.0793 ± 0.0016	0.7850	0.1448 ± 0.0033	0.1344 ± 0.0023
0.7629	0.1321 ± 0.0052	0.1186 ± 0.0014			
0.7890	0.1411 ± 0.0071	0.1365 ± 0.0071			

*Data obtained from Labuza (1963); a_w—water activity; X_{eq}—equilibrium moisture content; BSGL = Brewer's spent grain "Lager" style; BSGW = Brewer's spent grain "Weiss" style.

Table S2. Fitting parameters of the proposed models fitted to the adsorption data.

T (°C)	Model fit parameter				GAB					
	χ^2		R_{Adj}^2		X_m		C		k	
	BSGL	BSGW	BSGL	BSGW	BSGL	BSGW	BSGL	BSGW	BSGL	BSGW
5	<0.0001	<0.0001	>0.9989	>0.9978	0.0598 ± 0.0008 [a]	0,0564 ± 0.0007 [a]	76.1689 ± 8,1024 [a]	95.6266 ± 5.6434 [a]	0.9375 ± 0,0133 [c]	0.9372 ± 0,0026 [d]
10	<0.0001	<0.0001	>0.9966	>0.9973	0.0587 ± 0.0009 [b]	0,0501 ± 0.0007 [b]	70.2431 ± 5,8836 [a]	64.1169 ± 4.2140 [c]	0.9532 ± 0,0268 [bc]	0.9411 ± 0,0012 [cd]
20	<0.0001	<0.0001	>0.9976	>0.9971	0.0476 ± 0.0010 [c]	0,0439 ± 0.0010 [c]	65.5893 ± 4,8710 [a]	82.0667 ± 4.4213 [b]	0.9405 ± 0,0279 [c]	0.9626 ± 0,0017 [b]
30	<0.0001	<0.0001	>0.9953	>0.9959	0.0414 ± 0.0009 [d]	0,0424 ± 0.0015 [c]	56.0584 ± 0,6762 [b]	52.2692 ± 7.1122 [c]	0.9620 ± 0,0191 [b]	0.9527 ± 0,0023 [c]
40	<0.0001	<0.0001	>0.9955	>0.9989	0.0394 ± 0.0008 [e]	0,0368 ± 0.0015 [cd]	41.0072 ± 5,1709 [d]	42.8096 ± 4.6300 [d]	0.9668 ± 0,0154 [b]	0.9508 ± 0,0016 [c]
50	<0.0001	<0.0001	>0.9951	>0.9987	0.0382 ± 0.0009 [ef]	0,0358 ± 0.0012 [d]	46.8779 ± 3,180 [cd]	58.4730 ± 1.9991 [c]	0.9650 ± 0,0185 [b]	0.9674 ± 0,0032 [b]
60	<0.0001	<0.0001	>0.9986	>0.9984	0.0381 ± 0.0009 [f]	0,0344 ± 0.0015 [d]	50.4859 ± 0,9589 [c]	47.5695 ± 6.3506 [d]	0.9647 ± 0,0072 [b]	0.9623 ± 0,0029 [bc]
70	<0.0001	<0.0001	>0.9992	>0.9928	0.0350 ± 0.0017 [gh]	0,0336 ± 0.0007 [de]	41.3370 ± 8,0861 [d]	45.5037 ± 9.3990 [d]	0.9856 ± 0,0056 [a]	0.9784 ± 0,0087 [b]
80	<0.0001	<0.0001	>0.9986	>0.9970	0.0342 ± 0.0016 [h]	0,0316 ± 0.0010 [e]	44.8590 ± 2,4552 [d]	29.3419 ± 9.6171 [e]	0.9671 ± 0,0243 [b]	0.9857 ± 0,3088 [a]
90	<0.0001	<0.0001	>0.9988	>0.9953	0.0323 ± 0.0011 [i]	0,0296 ± 0.0015 [e]	36.5881 ± 4,3454 [d]	26.5033 ± 9.6250 [e]	0.9924 ± 0,0198 [a]	0.9933 ± 0,0288 [a]

T (°C)	Model fit parameter				Peleg							
	χ^2		R_{Adj}^2		k1		n1		k2		n2	
	BSGL	BSGW	BSGL	BSGW	BSGL	BSGW	BSGL	BSGW	BSGL	BSGW	BSGL	BSGW
5	<0,0004	<0,0002	>0,9913	>0,9947	0,1905 ± 0,0086 [a]	0,1823 ± 0,0011 [b]	0,6863 ± 0,0462 [bc]	0,7154 ± 0,0277 [b]	0,6609 ± 0,0150 [b]	0,6319 ± 0,0122 [ab]	10,9507 ± 0,8672 [b]	10,85396 ± 0,3301 [b]
10	<0,0002	<0,0004	>0,9948	>0,9883	0,1709 ± 0,0006 [b]	0,1640 ± 0,0016 [bc]	0,6104 ± 0,0145 [cd]	0,6544 ± 0,0121 [bc]	0,6419 ± 0,0216 [b]	0,5898 ± 0,0037 [abc]	10,3305 ± 0,1581 [b]	11,03914 ± 0,2898 [b]
20	<0,0001	<0,0004	>0,9973	>0,9901	0,1487 ± 0,0026 [c]	0,1934 ± 0,0040 [a]	0,5843 ± 0,0171 [cd]	0,9653 ± 0,0260 [a]	0,7631 ± 0,0099 [a]	0,7746 ± 0,0189 [a]	10,6220 ± 0,3106 [b]	15,87177 ± 0,1539 [a]
30	<0,0003	<0,0001	>0,9805	>0,9962	0,1625 ± 0,0074 [bc]	0,1158 ± 0,0029 [cd]	0,8174 ± 0,0435 [a]	0,5609 ± 0,0212 [cd]	0,6886 ± 0,0260 [b]	0,5681 ± 0,0089 [abc]	13,7195 ± 0,5953 [a]	9,77815 ± 0,1049 [bc]
40	<0,0002	<0,0003	>0,9866	>0,9877	0,1600 ± 0,0126 [bc]	0,1229 ± 0,0172 [bc]	0,8054 ± 0,0813 [ab]	0,6493 ± 0,1247 [bc]	0,7142 ± 0,0158 [b]	0,6420 ± 0,0802 [ab]	14,2883 ± 1,2963 [a]	12,28847 ± 2,1835 [ab]
50	<0,0001	<0,0001	>0,9928	>0,9973	0,1134 ± 0,0089 [d]	0,0984 ± 0,0024 [de]	0,5583 ± 0,0681 [d]	0,5032 ± 0,0141 [de]	0,6108 ± 0,0221 [b]	0,5578 ± 0,0121 [abc]	10,1945 ± 0,8947 [b]	9,35688 ± 0,0813 [bc]
60	<0,0001	<0,0001	>0,9969	>0,9956	0,0710 ± 0,0012 [ef]	0,0715 ± 0,0069 [fg]	0,3056 ± 0,0080 [e]	0,3382 ± 0,0218 [fg]	0,2605 ± 0,0048 [d]	0,2973 ± 0,0669 [cde]	4,3650 ± 0,2843 [c]	5,24487 ± 0,8753 [de]
70	<0,0001	<0,0001	>0,9949	>0,9841	0,0759 ± 0,0041 [e]	0,0739 ± 0,0113 [ef]	0,3653 ± 0,0251 [e]	0,4038 ± 0,0727 [ef]	0,3177 ± 0,0284 [c]	0,4485 ± 0,3201 [bcd]	5,4682 ± 0,6951 [c]	6,93974 ± 3,2180 [cd]
80	<0,0001	<0,0001	>0,9972	>0,9871	0,0619 ± 0,0026 [ef]	0,0671 ± 0,0006 [fg]	0,3037 ± 0,0211 [e]	0,3457 ± 0,0108 [fg]	0,2234 ± 0,0067 [d]	0,2116 ± 0,0355 [de]	4,1106 ± 0,3769 [c]	4,54046 ± 0,4724 [de]
90	<0,0001	<0,0001	>0,9833	>0,9824	0,0570 ± 0,0039 [f]	0,0517 ±0,0030 [g]	0,2795 ± 0,0286 [e]	0,2445 ± 0,0301[g]	0,1874 ± 2,9117 [d]	0,0895 ± 0,0190 [e]	9,9886 ± 0,5880 [b]	2,57859 ± 0,9859 [e]

T (°C)	Model fit parameter				Halsey			
	χ^2		R_{Adj}^2		h1		h2	
	BSGL	BSGW	BSGL	BSGW	BSGL	BSGW	BSGL	BSGW
5	<0,0013	<0,0014	>0,9703	>0,9685	100,7785 ± 3,4123 ^{a}	109,9410 ± 3,73512 ^{a}	2,0705 ± 0,0258 ^{a}	2,0598 ± 0,0152 ^{a}
10	<0,0009	<0,0005	>0,9796	>0,9842	95,0893 ± 5,4950 ^{a}	111,0600 ± 0,96505 ^{a}	1,9809 ± 0,0152 ^{a}	1,9583 ± 0,0205 ^{a}
20	<0,0009	<0,0002	>0,9791	>0,9953	62,4861 ± 0,8565 ^{bc}	66,1457 ± 2,36748 ^{c}	1,6912 ± 0,0147 ^{b}	1,6179 ± 0,0118 ^{c}
30	<0,0002	<0,0004	>0,9938	>0,9817	68,1800 ± 2,8454 ^{b}	86,4255 ± 2,58951 ^{b}	1,5784 ± 0,0252 ^{bc}	1,6654 ± 0,0071 ^{bc}
40	<0,0001	<0,0001	>0,9967	>0,9954	61,4784 ± 2,4874 ^{bc}	70,3180 ± 9,21605 ^{c}	1,4965 ± 0,0185 ^{cd}	1,4879 ± 0,0683 ^{d}
50	<0,0001	<0,0001	>0,9956	>0,9953	63,5037 ± 2,4484 ^{b}	71,3598 ± 2,44338 ^{c}	1,4732 ± 0,0288 ^{cd}	1,4918 ± 0,0211 ^{d}
60	<0,0001	<0,0001	>0,9952	>0,9897	65,4189 ± 1,3780 ^{b}	64,0747 ± 4,51147 ^{c}	1,4469 ± 0,0251 ^{cd}	1,4224 ± 0,0197 ^{d}
70	<0,0001	<0,0001	>0,9912	>0,9830	52,6045 ± 0,7288 ^{c}	65,6423 ± 4,09906 ^{c}	1,3926 ± 0,0514 ^{d}	1,3893 ± 0,0197 ^{d}
80	<0,0001	<0,0001	>0,9937	>0,9903	63,9464 ± 5,2241 ^{bc}	78,4494 ± 10,37276 ^{bc}	1,4223 ± 0,0279 ^{d}	1,4889 ± 0,0683 ^{d}
90	<0,0001	<0,0001	>0,9942	>0,9752	52,8949 ± 1,4638 ^{c}	68,8918 ± 3,56865 ^{c}	1,4765 ± 0,1416 ^{cd}	1,7746 ± 0,0773 ^{b}
T (°C)	Model fit parameter				Henderson			
	χ^2		R_{Adj}^2		H1		H2	
	BSGL	BSGW	BSGL	BSGW	BSGL	BSGW	BSGL	BSGW
5	<0,0007	<0,0007	>0,9836	>0,9844	5,3050 ± 0,0861 ^{c}	5,4940 ± 0,0786 ^{d}	0,8712 ± 0,0153 ^{c}	0,8656 ± 0,0071 ^{c}
10	<0,0008	<0,0007	>0,9815	>0,9794	5,3763 ± 0,1474 ^{c}	5,7604 ± 0,0313 ^{d}	0,8576 ± 0,0097 ^{c}	0,8481 ± 0,0118 ^{cd}
20	<0,0010	<0,0008	>0,9778	>0,9775	4,6470 ± 0,0336 ^{c}	4,7573 ± 0,0810 ^{d}	0,7351 ± 0,0090 ^{c}	0,6976 ± 0,0073 ^{de}
30	<0,0008	<0,0006	>0,9666	>0,9722	5,0740 ± 0,1274 ^{c}	5,7020 ± 0,0820 ^{d}	0,7130 ± 0,0184 ^{c}	0,7654 ± 0,0039 ^{cde}
40	<0,0009	<0,0009	>0,9598	>0,9593	4,9384 ± 0,1168 ^{c}	5,2169 ± 0,3768 ^{d}	0,6766 ± 0,0137 ^{c}	0,6679 ± 0,0445 ^{e}
50	<0,0007	<0,0006	>0,9562	>0,9603	5,1888 ± 0,1226 ^{c}	5,5030 ± 0,1187 ^{d}	0,6891 ± 0,0191 ^{c}	0,7020 ± 0,0144 ^{de}
60	<0,0002	<0,0002	>0,9296	>0,9364	26,1983 ± 3,6792 ^{ab}	27,0754 ± 1,8960 ^{c}	1,4755 ± 0,0415 ^{b}	1,4492 ± 0,0261 ^{b}
70	<0,0002	<0,0002	>0,9233	>0,9344	23,1512 ± 0,8312 ^{b}	29,8268 ± 2,7580 ^{bc}	1,4458 ± 0,0809 ^{b}	1,4448 ± 0,0319 ^{b}
80	<0,0001	<0,0001	>0,9381	>0,9425	28,6249 ± 3,0780 ^{a}	37,2506 ± 3,1406 ^{ab}	1,4253 ± 0,0429 ^{b}	1,5199 ± 0,0874 ^{b}
90	<0,0001	<0,0001	>0,9383	>0,9414	29,5000 ± 0,5000 ^{a}	43,3248 ± 2,7580 ^{a}	2,0563 ± 0,2174 ^{a}	2,5151 ± 0,1237 ^{a}

T (°C)	Model fit parameter				Oswin			
	χ^2		R_{Adj}^2		M		N	
	BSGL	**BSGW**	**BSGL**	**BSGW**	**BSGL**	**BSGW**	**BSGL**	**BSGW**
5	<0,0009	<0,0009	>0,9803	>0,9792	0,1261 ± 0,0014 ^{a}	0,1196 ± 0,0037 ^{a}	0,1261 ± 0,0014 ^{a}	0,0188 ± 0,0012 ^{c}
10	<0,0006	<0,0003	>0,9863	>0,9906	0,1184 ± 0,0025 ^{b}	0,1065 ± 0,0022 ^{b}	0,1184 ± 0,0025 ^{b}	0,0133 ± 0,0007 ^{c}
20	<0,0007	<0,0001	>0,9835	>0,9963	0,1039 ± 0,0013 ^{c}	0,0901 ± 0,0008 ^{c}	0,1039 ± 0,0013 ^{c}	0,0113 ± 0,0000 ^{c}
30	<0,0002	<0,0003	>0,9932	>0,9866	0,0837 ± 0,0014 ^{d}	0,0833 ± 0,0007 ^{c}	0,0837 ± 0,0014 ^{d}	0,0204 ± 0,0005 ^{c}
40	<0,0002	<0,0002	>0,9922	>0,9915	0,0779 ± 0,0008 ^{def}	0,0702 ± 0,0030 ^{d}	0,0779 ± 0,0008 ^{def}	0,0177 ± 0,0020 ^{c}
50	<0,0002	<0,0001	>0,9907	>0,9913	0,0738 ± 0,0020 ^{fg}	0,0707 ± 0,0012 ^{d}	0,0738 ± 0,0020 ^{fg}	0,0167 ± 0,0017 ^{c}
60	<0,0001	<0,0001	>0,9699	>0,9590	0,0806 ± 0,0025 ^{de}	0,0750 ± 0,0026 ^{d}	0,0806 ± 0,0025 ^{de}	0,0394 ± 0,0052 ^{a}
70	<0,0001	<0,0001	>0,9643	>0,9570	0,0772 ± 0,0007 ^{efg}	0,0695 ± 0,0005 ^{d}	0,0772 ± 0,0007 ^{efg}	0,0437 ± 0,0042 ^{a}
80	<0,0001	<0,0001	>0,9728	>0,9690	0,0715 ± 0,0024 ^{gh}	0,0693 ± 0,0003 ^{d}	0,0715 ± 0,0024 ^{gh}	0,0352 ± 0,0087 ^{ab}
90	<0,0001	<0,0001	>0,9643	>0,9609	0,0665 ± 0,0035 ^{h}	0,0604 ± 0,0050 ^{e}	0,0665 ± 0,0035 ^{h}	0,0238 ± 0,0084 ^{bc}

a-i The mean values in the same column not followed by the same letter differ significantly ($P < 0.05$). *Xm, C, k, k1, n1, k2, n2, M, N, h1, h2 H1 e H2* are constants of the models. T=temperature.